Impact of Wrong Ambiguity Fixing on GNSS Positioning

F. Meng

Geosciences & Remote Sensing
Delft University of Technology

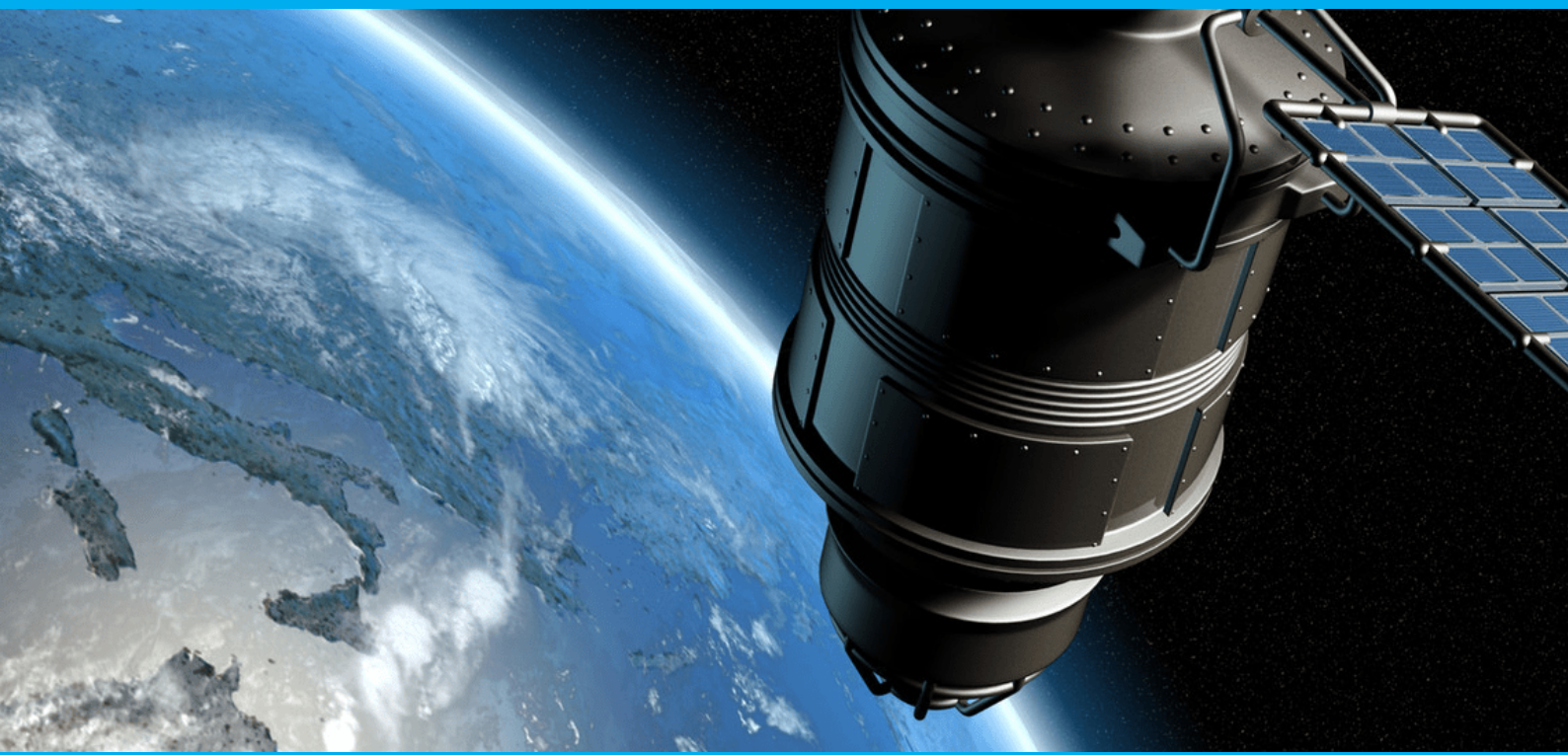

TU Delft

Impact of Wrong Ambiguity Fixing on GNSS Positioning

by

F. Meng

to finish the course AES4011-10 Additional Thesis
at the Delft University of Technology,

Student number:	4841204	
Project duration:	July 15, 2019 – October 31, 2019	
Thesis committee:	Dr. ir. A. A. (Sandra) Verhagen,	TU Delft, supervisor
	Dr. ir. W. (Wouter) van der Wal,	TU Delft

This thesis is confidential and cannot be made public until December 31, 2019.

TU Delft

Preface

This report was written by a Master student in Geosciences & Remote Sensing at Delft University of Technology, to summarize what he did during the project, as well as draw some conclusions. This report will also be assessed for the course AES4011-10 Additional Thesis.

I have heard about **LAMBDA** method, an ambiguity fixing method long before, and very interested in doing some research in it. It is a good chance for me to learn more about it by doing a small project. And I hope this report could be a bit helpful for other analyses in relative field.

While writing this report I assume readers have some basic knowledge of GNSS positioning, especially the phase measurement and ambiguity fixing. Readers could find more details about this project in Chapter 2 and Chapter 3.

I would like to thank my supervisor Dr. ir. A. A. (Sandra) Verhagen for her instructions and suggestions during this project and the scientific writing, and D. V. (Dimitrios) Psychas for his help for the programming of Kalman filter.

F. Meng
Delft, October 2019

Abstract

Global Navigation Satellite System (GNSS) has been developed in recent several decades, which provides a new technique for timing, positioning and navigation. And GNSS positioning is a basic service to us, both in daily life and scientific research. During high-precise positioning, ambiguity resolution is a key factor that has a huge influence on the accuracy of the result. And the wrong fixing is the main source of lose of accuracy, so many methods of test are proposed to validate the fixing result. We are interested in the performance of solutions that have been labeled as wrong fixing, and want to check if those wrong fixings should be excluded or accepted during estimation.

At first we introduce the basic model and challenges of ambiguity fixing, as well as the widely used method integer least squares and Z-transformation. Some previous research of distribution of fixed solution also enables us to compute the bounds of baseline residual. Then we focus on an example to do some pre-research, and find out the main research question - how to accept wrong fixing during estimation and the impact under different scenarios or estimation methods. We use a simulation-based method to do the research but the measurements are generated based on the real ephemeris in certain day.

After giving the double difference measurement model based on code and phase with respect to single or dual frequencies, in short baseline scenario, we define some parameters 1-norm, infinity-norm, weighted 2-norm, and good/bad performance of wrong fixings that might be useful for analysis. And some detailed information in chosen epochs are shown with multiple figures and we derive those which are helpful, such as infinity-norm ratio. Then we develop 4 validation methods, **Infinity-norm ratio detection** (**RD**), **Weighted 2-norm detection** (**WD**), **1-norm baseline residual detection** (**BD1**) and **Infinity-norm baseline residual detection** (**BDi**), to check if we could recognize wrong fixings with good performance from all wrong fixings. We also compute some statistics, such as **the success rate of detection**, **the rate of misdiagnose**, and **the rate of participation** to see whether our validation methods are effective or not. The histogram of wrong fixing or correct fixing corresponds the existed research of distribution well. And the time series analysis also proves the reliability of our validation methods, although there exist some errors due to the small sample size of simulations.

We also apply the multi-epoch least squares and Kalman filter to see the influence of fixing success rate, standard deviation of horizontal residuals, residual bounds and performance of wrong fixings. We find that there are obvious improvements on all of them. An extra experiment is designed to see the impact of atmospheric delays and the results show that it is really different from short baseline scenarios and we need to find more proper threshold to make sure our validation methods work.

Finally, we could draw a conclusion that it is possible to find out wrong fixings that could be accepted, but the threshold for each validation method should be adaptive for different scenarios and Kalman filter is very reliable, with which the wrong fixing is always likely to be excluded during the estimation.

Keywords: **GNSS DD positioning, ambiguity fixing, wrong fixing, validation method, Kalman filter, time series analysis.**

Contents

1 Introduction

GNSS is the main technique that provides geospatial positioning to us, to help people know where they are when travelling to a strange environment, or to monitor minor deformation and motion of manual or natural objects on earth, etc. While during the communication between the satellite and the receiver, there exist different kinds of errors or delays in signal transmission, which has a large influence on our positioning result if we wrongly estimate them. In addition, some parameters could help the research in other fields, i.e. atmospheric delays could be applied to estimate water vapor content. So we always try to precisely estimate each parameter before analysis.

1.1. GNSS Carrier-Phase Ambiguities

In GNSS positioning we could use two kinds of observations: code measurement and carrier-phase measurement. Estimation using carrier-phase measurement, the residual of which could be in millimeters, is much more precise than that using pseudoranges, but we need to fix the ambiguity for every satellite with respect to the receiver per frequency since we do not know how many cycles the carrier wave has traveled for during the journey:

$$\Phi = \lambda N + \varphi \tag{1.1}$$

where Φ is total phase [m], λ is wavelength [m], N is phase ambiguity [cycles] and φ is phase measurement [m], i.e. the fractional phase.

Relative positioning is one of general positioning methods which could help us eliminate or mitigate different kinds of errors during estimation. In double difference (**DD**) relative positioning, with least-squares or Kalman filter we estimate the phase ambiguity as a float, but in fact it is an integer. So it is important to do the ambiguity resolution (**AR**) during the GNSS processing[3], which could fix the float solution and remarkably improve the precision of the result.

The general model for **DD** positioning could be shown as

$$\Phi^{kl}_{ur,f} = \varphi^{kl}_{ur,f} - \gamma_f I^{kl}_{ur,f_0} + T^{kl}_{ur,f} + \lambda N^{kl}_{ur,f} + \epsilon^{kl}_{ur,f} \tag{1.2}$$

with subscripts ur as user and reference station, f, f_0 as the frequency and the reference frequency, respectively; and superscripts kl as satellite PRN k and l, γI as ionosphere delay where $\gamma = f_0^2 / f^2$, T as troposphere delay, ϵ as phase noise.

To fix the ambiguity N, we apply a mixed-integer GNSS model with normally distributed measurements $\mathbf{y}$:

$$\mathbf{y} \sim N(\mathbf{Ax}, \mathbf{Q_{yy}}), \quad \mathbf{x} = \begin{bmatrix} \mathbf{b} & \mathbf{a} \end{bmatrix}^{\mathrm{T}}, \mathbf{a} \in \mathbb{Z}^n, \mathbf{b} \in \mathbb{R}^m \tag{1.3}$$

with $\mathbf{A}$ the design matrix, $\mathbf{a}$ ambiguity vector [m] with n parameters and $\mathbf{b}$ parameter vector with m parameters.

There are four main steps in **AR** [3]:

1. **Float Solution**: we neglect the integer nature of ambiguities and apply a standard least squares (**LS**) to achieve the float solution $\hat{\mathbf{a}}$, $\hat{\mathbf{b}}$, $\mathbf{a}, \mathbf{b} \in \mathbb{R}^{m+n}$.

2. **Integer Solution**: in terms of the float solution $\hat{\mathbf{a}}$, it could be fixed to integer solution $\check{\mathbf{a}}$ which is within integer nature, under certain algorithm such as integer rounding (**IR**), integer bootstrapping (**IB**), etc.

3. **Validation**: after the fixing of ambiguities, we need to validate the solution by a testing function under certain threshold, to see whether we could accept the fixed solution or not.

4. **Fixed Solution**: once the integer solution $\check{\mathbf{a}}$ is accepted, the residual between float solution and integer solution ($\hat{\mathbf{a}}-\check{\mathbf{a}}$) could be used for the estimation of fixed parameter $\check{\mathbf{b}}$, together with variance-covariance matrix:

$$\check{\mathbf{b}}|\hat{\mathbf{a}} = \hat{\mathbf{b}} - \mathbf{Q}_{\hat{\mathbf{b}}\hat{\mathbf{a}}}\mathbf{Q}_{\hat{\mathbf{a}}\hat{\mathbf{a}}}^{-1}(\hat{\mathbf{a}}-\check{\mathbf{a}}) \tag{1.4}$$

$$\mathbf{Q}_{\check{\mathbf{b}}\check{\mathbf{b}}} = \mathbf{Q}_{\hat{\mathbf{b}}\hat{\mathbf{b}}} - \mathbf{Q}_{\hat{\mathbf{b}}\hat{\mathbf{a}}}\mathbf{Q}_{\hat{\mathbf{a}}\hat{\mathbf{a}}}^{-1}\mathbf{Q}_{\hat{\mathbf{a}}\hat{\mathbf{b}}} \tag{1.5}$$

Finally, we get a highly precise vector of parameters. And in short-baseline positioning where we neglect atmospheric delays, it is so-called baseline vector.

So if we want to get a satisfactory result, it significantly depends on the correctness of our integer solution.

1.2. Integer Least-Squares (ILS) and Z-transformation

Based on (1.3) we could apply a mixed integer least-squares, which is a non-standard least-squares problem due to $\mathbf{a} \in \mathbb{Z}^m$ [7]:

$$\left(\check{\mathbf{a}}_{LS},\quad \check{\mathbf{b}}_{LS}\right) = \underset{\mathbf{a}\in\mathbb{Z}^m,\,\mathbf{b}\in\mathbb{R}^n}{\arg\min}\ \|\mathbf{y}-\mathbf{A}\mathbf{x}\|^2_{\mathbf{Q}_{\mathbf{yy}}} \tag{1.6}$$

$$\begin{aligned}\check{\mathbf{a}}_{LS} &= \underset{\mathbf{z}\in\mathbb{Z}^m}{\arg\min}\ \|\hat{\mathbf{a}}-\mathbf{z}\|^2_{\mathbf{Q}_{\hat{\mathbf{a}}\hat{\mathbf{a}}}}\\ \check{\mathbf{b}}_{LS} &= \hat{\mathbf{b}} - \mathbf{Q}_{\hat{\mathbf{b}}\hat{\mathbf{a}}}\mathbf{Q}_{\hat{\mathbf{a}}\hat{\mathbf{a}}}^{-1}(\hat{\mathbf{a}}-\check{\mathbf{a}}_{LS})\end{aligned} \tag{1.7}$$

An $n\times n$ matrix $\mathbf{Z}$ is called a Z-transformation if $\mathbf{Z},\mathbf{Z}^{-1}\in\mathbb{Z}^{n\times n}$ [9]. It is a method of reparameterization. For **IR** and **IB** we do not need a search since after Z-transformation the integer solution is not invariant, although it has higher success rate afterwards. Instead for **ILS** the Z-transformation is needed for a different purpose: the decorrelation will ensure a higher success rate. Besides, the searching space is usually very elongated during integer fixing, which is time consuming, while Z-transformation is a ideal way to shorten the search time of $\hat{\mathbf{a}}$, with $\hat{\mathbf{z}} = \mathbf{Z}\hat{\mathbf{a}}$. A general method is called decorrelating transformation, which has a good performance in any integer GNSS model [4, 8, 10]. It is controlled by a sequence of matrices for the alternating reduction in different dimensions and the final correlation would be smaller than 0.5.

We have mentioned two methods of integer estimation **IR** and **IB**, but both of them suffer a lot from the lack of Z-transformation invariance, while for **ILS**, the variance-covariance matrix of $\hat{\mathbf{z}}$ is equal to $\hat{\mathbf{a}}$ ($\|\mathbf{Q}_{\hat{\mathbf{z}}\hat{\mathbf{z}}}\| = \|\mathbf{Q}_{\hat{\mathbf{a}}\hat{\mathbf{a}}}\|$), which is Z-transformation invariant [3]. So after Z-transformation, the estimation of **ILS** is the same as that without transformation.

And due to the fact that **ILS** is Z-invariant:

$$\begin{aligned}\check{\mathbf{z}}_{LS} &= \mathbf{Z}\check{\mathbf{a}}_{LS}\\ \check{\mathbf{b}}_{LS} &= \hat{\mathbf{b}} - \mathbf{Q}_{\hat{\mathbf{b}}\hat{\mathbf{z}}}\mathbf{Q}_{\hat{\mathbf{z}}\hat{\mathbf{z}}}^{-1}(\hat{\mathbf{z}}-\check{\mathbf{z}}_{LS})\end{aligned} \tag{1.8}$$

with $\mathbf{Q}_{\hat{\mathbf{b}}\hat{\mathbf{z}}} = \mathbf{Q}_{\hat{\mathbf{b}}\hat{\mathbf{a}}}\mathbf{Z}^{\mathrm{T}}$ and $\mathbf{Q}_{\hat{\mathbf{z}}\hat{\mathbf{z}}} = \mathbf{Z}\mathbf{Q}_{\hat{\mathbf{z}}\hat{\mathbf{z}}}\mathbf{Z}^{\mathrm{T}}$.

In terms of integer fixing in **ILS**, a general procedure is described as **LAMBDA** (**L**east-squares **AMB**iguity **D**ecorrelation **A**djustment) method [10]. And through this method the success rate of fixing is higher than **IR** and **IB**:

$$P(\check{\mathbf{a}}_{LS}=\mathbf{a}) \geq P(\check{\mathbf{a}}_{B}=\mathbf{a}) \geq P(\check{\mathbf{a}}_{R}=\mathbf{a}) \tag{1.9}$$

Although the success rate of **IB** and **IR** is not as high as **ILS**, it could still be applied during the fixing. Especially for **IB**, its success rate could perform as the lower bound for **ILS**, which is generally used as the best known lower bound [14].

In practice, sometimes due to the fact of poor environment leading to a unreliable solution, we might not fix all ambiguities, but a subset, which is referred as partial ambiguity resolution (**PAR**) [5]. Besides, the fixing procedure could be controlled by a test, such as the fixed failure-rate approach [6].

1.3. Fixed Solution

There is a lot of research about the quality of GNSS parameters, especially fixed baseline estimation. In general the distribution of the float baseline solution is assumed as normal distribution[14], i.e. $\hat{\mathbf{b}} \sim N(\mathbf{b}, \mathbf{Q}_{\hat{\mathbf{b}}\hat{\mathbf{b}}})$, and its probability density function (**PDF**) together with conditional **PDF** based on (1.4), (1.5) and (1.8):

$$\begin{aligned} f_{\hat{\mathbf{b}}}(\mathbf{x}) &= \frac{1}{\sqrt{|\mathbf{Q}_{\hat{\mathbf{b}}\hat{\mathbf{b}}}|(2\pi)^{0.5p}}} exp\{-\frac{1}{2} \ \|\mathbf{x}-\mathbf{b}\|^2_{\mathbf{Q}_{\hat{\mathbf{b}}\hat{\mathbf{b}}}}\} \\ f_{\hat{\mathbf{b}}|\hat{\mathbf{a}}}(\mathbf{x}|\mathbf{z}) &= \frac{1}{\sqrt{|\mathbf{Q}_{\hat{\mathbf{b}}|\hat{\mathbf{a}}}|(2\pi)^{0.5p}}} exp\{-\frac{1}{2}\|\mathbf{x}-\mathbf{b}|\mathbf{z}\|^2_{\mathbf{Q}_{\hat{\mathbf{b}}|\hat{\mathbf{a}}}}\} \end{aligned} \tag{1.10}$$

After the baseline vector is fixed, the distribution could be derived as [11, 13]:

$$f_{\check{\mathbf{b}}}(\mathbf{x}) = \sum_{\mathbf{z}\in\mathbb{Z}^n} f_{\hat{\mathbf{b}}|\hat{\mathbf{a}}}(\mathbf{x}|\mathbf{z}) P(\check{\mathbf{a}} = \mathbf{z}) \tag{1.11}$$

As for the conditional variance-covariance matrix, it could be used to find the bounds of baseline residual [12]:

$$\begin{aligned} &P(\hat{\mathbf{b}}|\hat{\mathbf{a}} \in E_{\mathbf{b}}) P(\check{\mathbf{a}} = \mathbf{a}) \le P(\check{\mathbf{b}} \in E_{\mathbf{b}}) \le P(\hat{\mathbf{b}}|\hat{\mathbf{a}} \in E_{\mathbf{b}}) \\ &E_{\mathbf{b}} = \{\mathbf{x} \in \mathbb{R}^n | (\mathbf{x}-\mathbf{b})^{\mathrm{T}} \mathbf{Q}^{-\mathbf{1}}_{\hat{\mathbf{b}}|\hat{\mathbf{a}}} (\mathbf{x}-\mathbf{b}) \le \beta^2\} \end{aligned} \tag{1.12}$$

with $E_{\mathbf{b}}$ the confidence region of baseline parameter.

The selection of β comes from the lower and upper bounds:

$$\alpha_1 \le P(\|\check{\mathbf{b}} - \mathbf{b}\|^2_{\mathbf{Q}_{\hat{\mathbf{b}}|\hat{\mathbf{a}}}} \le \beta^2) \le \alpha_2 \tag{1.13}$$

with $\alpha_1 = \alpha_2 P(\check{\mathbf{a}} = \mathbf{a})$ and $\alpha_2 = P(\chi^2(p,0)) \le \beta^2$ [14].

(1.13) could be used for detection of whether our fixed solution is confident or not. If the success rate is high enough, the bounds would be tight. Besides, there are some other probabilities for evaluation such as $P(\|\check{\mathbf{b}} - \mathbf{b}\|^2_{\mathbf{Q}_{\check{\mathbf{b}}\check{\mathbf{b}}}} \le \beta^2)$ and $P(\|\hat{\mathbf{b}} - \mathbf{b}\|^2_{\mathbf{Q}_{\hat{\mathbf{b}}\hat{\mathbf{b}}}} \le \beta^2)$.

1.4. Reasearch Objectives

We have derived the expression of distribution of fixed baseline parameter, although we do not know the exact kind of distribution it has. In practice, there are always some solutions that are wrongly fixed, when the property of these solutions would not meet what we have retrieved before. The distribution of these wrong fixings are so random that we cannot describe it by a simple function, and they are rejected by the test for validation, but some of them could be accepted because of small error, as Figure 1.1 which is an example in certain scenario shows:

Some clusters still have estimation errors which are small compared to the 95% confidence region of the float solution, which means that some of them might be accepted in estimation. While it is just a simple case, the information we have retrieved is very limited from a plot of horizontal residuals, and it would be especially severe if the fixed estimation errors are larger than those of the float. So furthermore, we need to do some pre-research to check if there exist wrong fixings that could be accepted. We compute some statistics, that among these 10^6 samples, the success rate for fixing is equal to 93.51%, with 6.49% of all samples generated as wrong fixings. And for these wrong fixings, 52% of them have small horizontal errors ($|\check{\mathbf{b}}_{w,N} - \mathbf{b}_N| + |\check{\mathbf{b}}_{w,E} - \mathbf{b}_E| \le 0.1m$), where $\check{\mathbf{b}}_w$ is wrongly fixed baseline in north (N) and east (E), $\mathbf{b}$ is the true baseline. It is a large number for candidates of the wrong fixing that might be accepted, while we need to find some proper methods for validation; and in different scenarios, there might be some changes of distribution and range for wrong fixings.

As a result, it is really necessary to do some research, to check the bounds of float or fixed solutions, **and how many wrong fixings could be accepted in various scenarios as well as how to accept them.** Even we must consider about these questions, usually the size of wrong fixings is very small, how could we effectively retrieve the feature of wrongly fixed solutions for validation? **And if we use different parameters or estimation methods, is there any improvement or influence for the validation?**

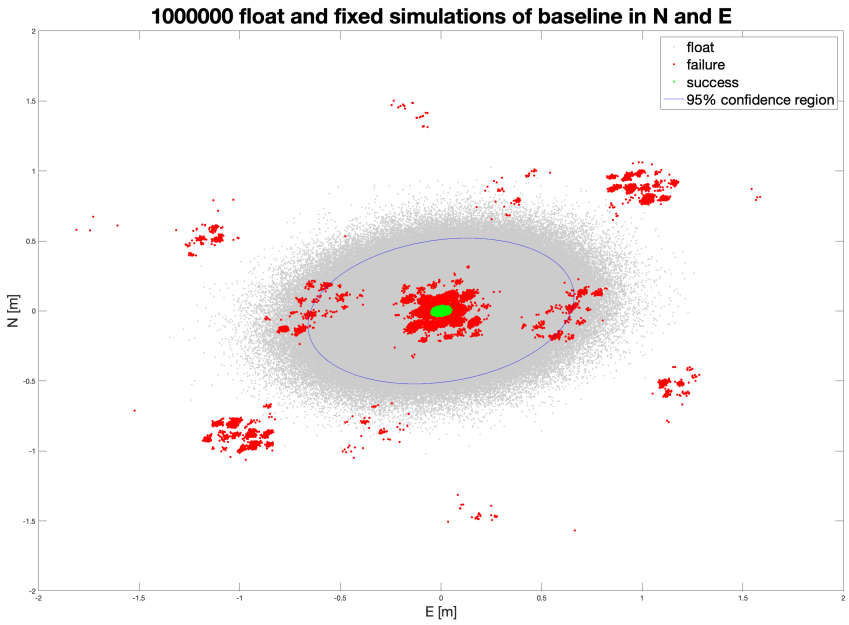

Figure 1.1: Horizontal residuals for float and fixed solutions based on simulations. Grey: float solutions; red: wrong fixings; green: successful fixings

1.5. Methodology and Dataset

Since there are different kinds of errors and delays in the measurement, we cannot only focus on the ambiguity by removing the influence of other parameter. As a result, it would be more proper to apply a **simulation-based** method, that we use a 'Q_GUI' (Figure 1.2) in LAMBDA_v3.0 toolbox[1] to generate our measurements under certain circumstance with real ephemeris in certain period, given standard deviation of code and phase, the location of the receiver, frequency and system combinations, time interval and number of epochs, satellite's cutoff elevation, atmospheric corrections and mapping function. Based on the defined scenario and model, we could estimate the parameter we need, including the variance-covariance matrix for float or fixed baseline solutions. After that, we could simulate the float solutions with large enough samples based on variance-covariance matrix under standard normal distribution, and fix them by **LAMBDA** method, which means we assume the true value to be equal to zero for both ambiguities and other parameters or the date is detrended. Finally, we could do some analysis based on the float and fixed solutions.

We select one-day ephemeris in 10th May 2019 with static receiver in $(52,4,0)$ (latitude [deg] longitude [deg] height [m]) to analyse the distribution of fixings in different epochs under GPS, as well as time analysis for the whole day to avoid some accident results. As for the potential factors that might affect the fixed simulations, they are more likely to be other unknown parameters such as troposphere delay and ionosphere delay, and the number of frequencies which would change the number of ambiguities since they are more or less correlated with each other. While for the date we choose and the location of the receiver, they might not, and in this report we only concentrate on the ambiguities of GPS satellites. As for the unit in this report, if not mentioned, it would be in meters.

Figure 1.2: Integer Ambiguity Resolution Demo Q_GUI

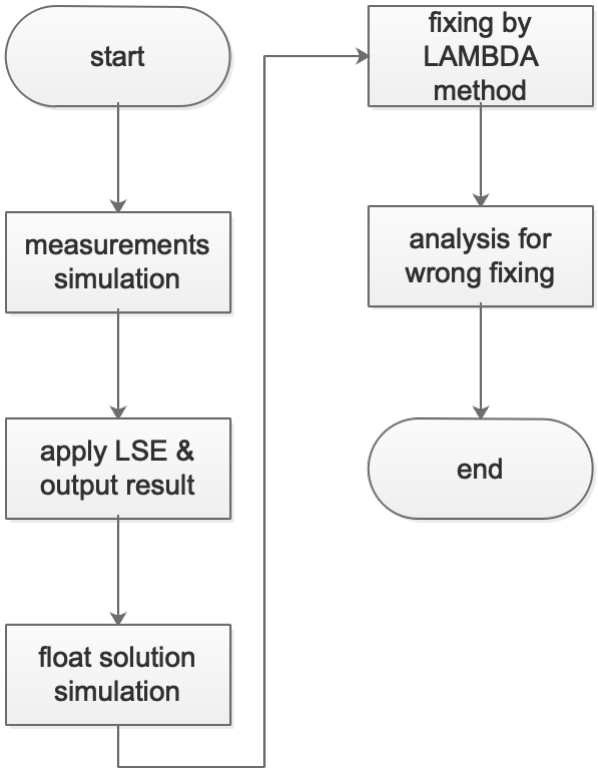

Figure 1.3: A simple flowchart of processing

2

Wrong Fixing under Least-Square Estimation (LSE)

LSE is one of the most common methods during the GNSS positioning. It is easy to implement, and the more measurements, the more precise the estimation. The output for Q_GUI is a sequence of results including variance-covariance matrix, lower bound of success rate, observable satellite numbers, etc. for each epoch, computed based on the environment on these epochs, so we could focus on each epoch to analyse the performance of the wrong fixing.

2.1. Short-baseline Scenario

The basic model of short-baseline positioning could be described as:

$$\begin{bmatrix} \delta\mathbf{P}_{t=i;L1} \\ \delta\mathbf{\Phi}_{t=i;L1} \end{bmatrix} = \begin{bmatrix} \mathbf{U}_{t=i} & \mathbf{O} \\ \mathbf{U}_{t=i} & \mathbf{\Lambda}_{L1} \end{bmatrix} \begin{bmatrix} \delta\mathbf{x}_{ur} \\ \mathbf{a}_{L1} \end{bmatrix} \tag{2.1}$$

$$\begin{bmatrix} \delta\mathbf{P}_{t=i;L1} \\ \delta\mathbf{\Phi}_{t=i;L1} \\ \delta\mathbf{P}_{t=i;L5} \\ \delta\mathbf{\Phi}_{t=i;L5} \end{bmatrix} = \begin{bmatrix} \mathbf{U}_{t=i} & \mathbf{\Lambda}_{L1} & \mathbf{O} \\ \mathbf{U}_{t=i} & \mathbf{O} & \mathbf{\Lambda}_{L5} \end{bmatrix} \begin{bmatrix} \delta\mathbf{x}_{ur} \\ \mathbf{a}_{L1} \\ \mathbf{a}_{L5} \end{bmatrix} \tag{2.2}$$

for single and dual frequencies, with $L1$ and $L5$ the frequencies, $\delta\mathbf{P}_{t=i}$ and $\delta\mathbf{\Phi}_{t=i}$ **DD** code and phase measurements [m], $\mathbf{U}_{t=i}$ **DD** line of sight (**LOS**) matrix in epoch i, $\mathbf{\Lambda}$ matrix of wavelength, $\delta\mathbf{x}_{ur}$ baseline vector [m] and $\mathbf{a}$ unknown **DD** ambiguities. We could neglect the troposphere and ionosphere delays in short-baseline.

The variance-covariance matrix $\mathbf{Q}_{\mathbf{yy},f}$ for the measurement with combination of code and phase under certain frequency f and weight matrix $\mathbf{W}$, based on the elevation angle with 15-degree cutoff value could be computed from (2.3)

$$\begin{aligned} &\sigma_{i,P,f} = 2\sigma^2_{P_{0,f}}(1+10exp\{-\alpha_i/10\})^2 \\ &\sigma_{i,C,f} = 2\sigma^2_{C_{0,f}}(1+10exp\{-\alpha_i/10\})^2 \\ &\mathbf{Q}_{C,f} = diag(w_{1,C,f}, w_{2,C,f}, ..., w_{n,C,f}) \\ &\mathbf{Q}_{P,f} = diag(w_{1,P,f}, w_{2,P,f}, ..., w_{n,P,f}) \\ &\mathbf{Q}_{\mathbf{yy},f} = diag(\mathbf{T}\mathbf{W}_{C,f}\mathbf{T}^{'}, \mathbf{T}\mathbf{W}_{P,f}\mathbf{T}^{'}) \\ &\mathbf{W} = \mathbf{Q}_{\mathbf{yy}}^{-1} \end{aligned} \tag{2.3}$$

where C and P represent code and phase, respectively, σ is the standard deviation, α is elevation angle and $\mathbf{T}$ is the transformation matrix for **DD** model. For n satellites, there are $2N(n-1)$ weights for N frequencies. In addition, we use the satellite with maximum elevation as our reference satellite for each epoch.

As a result, the estimated variance-covariance matrix of baseline and ambiguities could be retrieved by:

$$\begin{bmatrix} \mathbf{Q}_{\hat{\mathbf{b}}\hat{\mathbf{b}}} & \mathbf{Q}_{\hat{\mathbf{b}}\hat{\mathbf{a}}} \\ \mathbf{Q}_{\hat{\mathbf{a}}\hat{\mathbf{b}}} & \mathbf{Q}_{\hat{\mathbf{a}}\hat{\mathbf{a}}} \end{bmatrix} = (\mathbf{A}^{\mathrm{T}}\mathbf{W}\mathbf{A})^{-1} \tag{2.4}$$

with **A** the design matrix based on (2.1) or (2.2).

Following the Flowchart 1.3 and we could get our simulations finally.

2.2. Validation for the Wrong Fixing

Before doing the validation for wrong fixings we start to focus on single epoch to see the details of our samples, including the horizontal residuals and the performance of the wrong fixing under different defined parameters.

For a sample $\underline{\mathbf{x}}$, since there are many parameters inside the vector, we define three main parameters to describe its error in general, comparing with the true value: **1-norm** $\|\underline{\mathbf{x}}-\mathbf{x}\|_1$ which shows the overall residual of baseline parameters, weighted **2-norm** $\|\underline{\mathbf{x}}-\mathbf{x}\|^2_{\mathbf{Q}_{\underline{\mathbf{xx}}}}$ which shows the overall residual of baseline parameters under weights and **infinity-norm** $\|\underline{\mathbf{x}}-\mathbf{x}\|_\infty$ which shows the maximum residual of baseline parameters. And we also define the good performance and bad performance in case of wrong fixings:

$$good\ performance = |\check{\mathbf{b}}_{w,N}-\mathbf{b}_N| \leq 3\sigma_{\check{\mathbf{b}}_N}\ \&\ |\check{\mathbf{b}}_{w,E}-\mathbf{b}_E| \leq 3\sigma_{\check{\mathbf{b}}_E}\ \&\ |\check{\mathbf{b}}_{w,U}-\mathbf{b}_U| \leq 3\sigma_{\check{\mathbf{b}}_U} \tag{2.5}$$

where $\check{\mathbf{b}}_w$ is the wrong fixing of baseline in north (N), east (E) and up (U) direction, $\mathbf{b}$ is the true baseline and $\check{\mathbf{b}}$ is correct fixing with σ as its standard deviation computed from samples of correct fixings. For performance of the wrong fixing other than good performance is defined as bad performance.

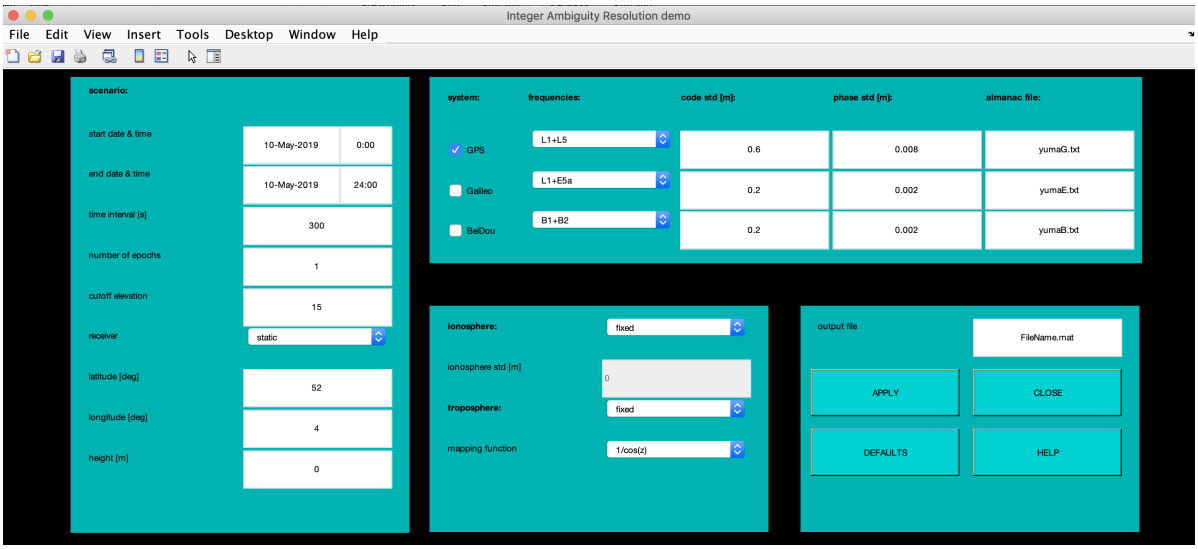

Figure 2.1: Selection of parameters in Q_GUI

We randomly choose six epochs 1, 70, 112, 186, 229, 285 [$\times 5min$] (to simplify we assume for each epoch the circumstance of observation does not change), which is approximately uniformly distributed during the day, to simulate and visualize scenarios for single and dual frequencies, with 10^6 samples. And we choose a 0.6 m standard deviation of code and 8 mm of phase to make sure the failure rate is 'high' enough in some epochs to generate enough $\check{\mathbf{b}}_w$ for analysis, as Figure 2.1 shows. Since it is based on short-baseline, the atmospheric delay is fixed. For example, some figures we plot for epoch 285 with dual frequencies could be shown as Figure 2.2 to 2.6, when there are 9 satellites, with -0.14 correlation between north and east:

Similar to Figure 1.1, we could retrieve some information from Figure 2.2 as well, when the success rate of fixing is equal to 91.34% and failure rate is equal to 8.66%. The distribution of the wrong fixing in epoch 285 is much more random than the previous plot, but there are still many small clusters. And it would be severe that many clusters are outside the 95% confidence region. The residual of correct fixing is so small that we could only figure out a small cluster in the center, while the region of float solutions is much larger, showing that after fixing there is a huge improvement for horizontal baseline parameters. As for the performance of wrong fixings, it is too random to see whether there exist wrong fixings with good performance or not. We suppose the horizontal correlation might have an impact on the horizontal distribution of wrong fixings, while in this scenario the failure rate is not very high, so it shows a more random distribution than we expect.

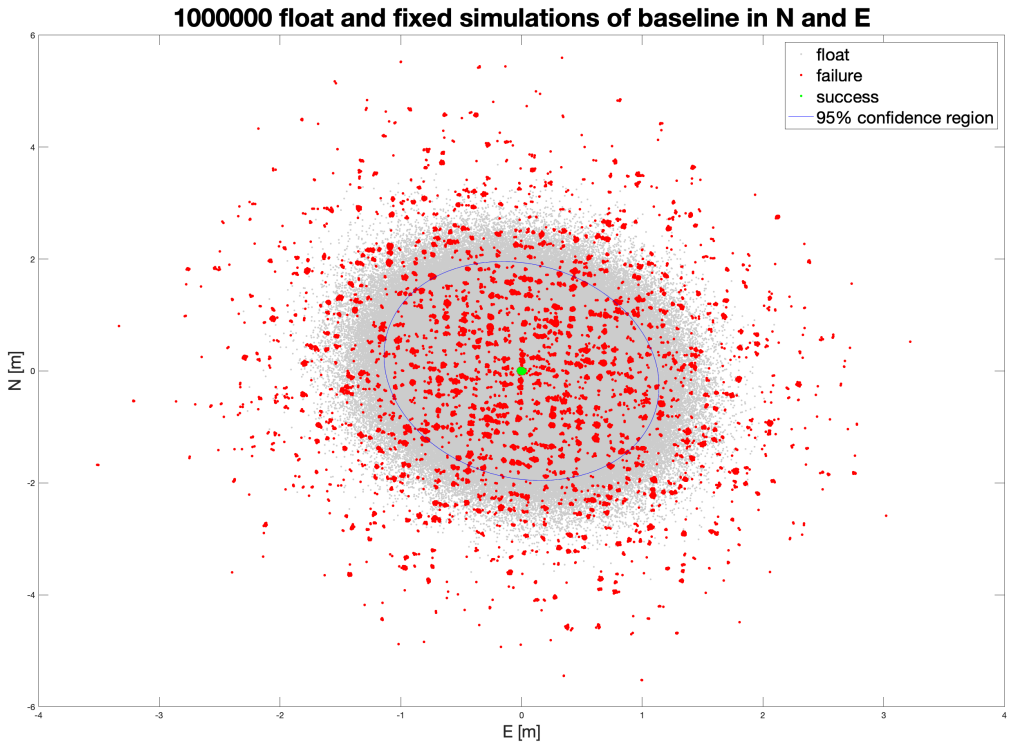

Figure 2.2: Horizontal residuals for float and fixed solutions based on simulations in epoch 285. Grey: float solutions; red: wrong fixings; green: successful fixings

The influence of horizontal correlation is more clear in figures shown in Section 3.3, where we could observe a more correlated clusters in horizontal.

Besides, in this epoch, there are $2 \times (9-1) = 16$ unknown ambiguities and three baseline parameters. We cannot show their residuals separately, while it would be a proper way to use 1-norm or infinity norm to represent the 'overall residual' of the ambiguity or baseline. And we could create a joint histogram between them, only for wrong fixings, shown as Figure 2.3. It is reasonable to see that the overall residual of baseline increases with that of ambiguity, based on (1.4) and (1.5). And the top two plots of Figure 2.4 could show it more obviously, where the scatter plot is like a comet. In terms of the plot of 1-norm residual, it seems that the ratio between ambiguity and baseline is fluctuated around a constant, while we could see an offset in scatter plot of infinity-norm. For a large ratio, it means that a smaller residual of ambiguities could lead to a relatively large error of baseline parameters. These two visualizations are shown as bottom two plots of Figure 2.4.

In the ratio plot, we separate the wrong fixing by good and bad performance. And these plots correspond what we mentioned before. The ratio of 1-norm fluctuates a lot around 0.05 for wrong fixings with both good and bad performance. While the distribution of the wrong fixing with good performance distinguish a lot from bad performance. In this case most values of wrong fixings with good performance are below around 0.55. But because of the large size of sample, there are many overlaps in the boundary between red and green dots, and we need to do some computations to see if there is a clear threshold that could well recognize good performance from wrong fixings.

Figure 2.5 gives another potential method of validation for the wrong fixing, which is based on the norm of baseline or ambiguity residuals. If we find a proper threshold the separation would be good enough. But due to the large range of these parameters, the threshold might change over time or under different circumstances. For another norm, weighted 2-norm we visualize the residual for both float and fixed solutions, as well as that for good and bad performance separately among wrongly fixed solutions in Figure 2.6. We could see that the former is not a good factor for validation since wrong fixings with good performance and bad performance have large overlaps of range. But for the later, if the wrong fixing has bad performance, the 2-norm would be very large, whose value could reach 10^5. So there could also be a threshold for validation. Besides, the stripes in the figures could correspond the clusters in Figure 2.2 well, since both $\check{\mathbf{a}}$ and $\mathbf{a}$ must be integers, and fixed baseline parameters are corrected from fixed ambiguities.

For the visualizations in other 5 epochs, all of them show something in common with what we mentioned

above. But in some epochs there are not wrong fixings with good performance, which is possible because the distribution of wrongly fixed estimation is very random, and what we should do first is to find a good validation method to recognize these good performances. In addition, the result of single frequency under the same circumstance is much worse than dual frequencies, and the interesting thing is that results of all epochs we choose for the scenario of single frequency do not show any good performance among wrong fixings. We will mention it in Section 3.1 by applying a simple multi-epoch **LSE**. And we would use a smaller standard deviation for single frequency for Section 2.4 time series analysis to check our validation method.

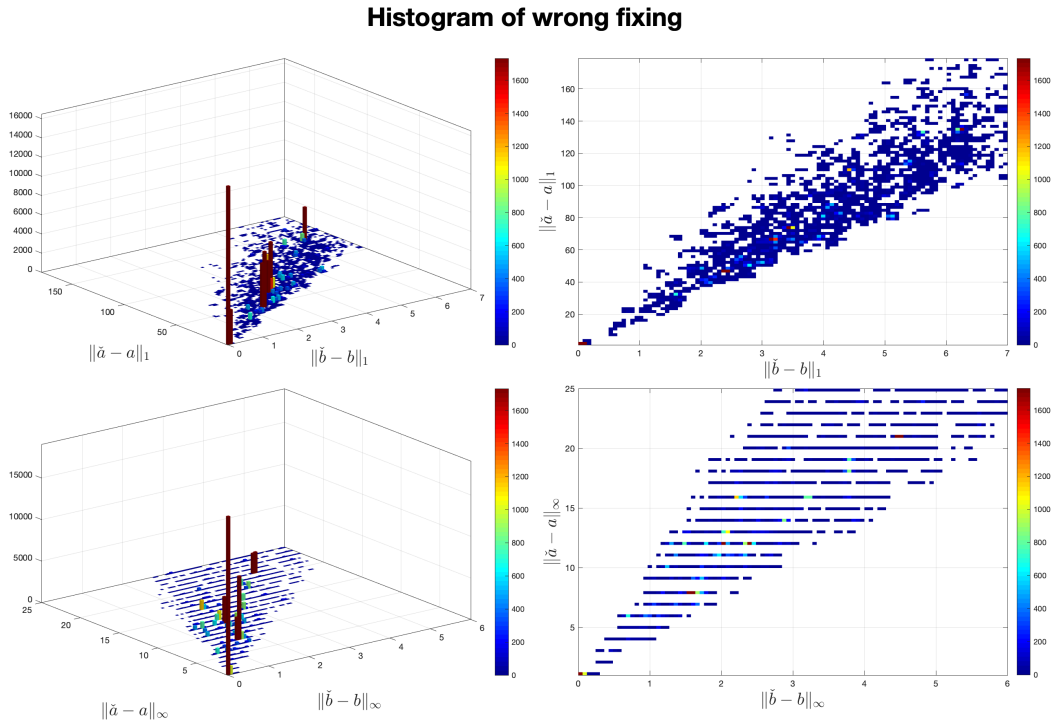

Figure 2.3: Histogram of wrongly fixed ambiguity (y-axis) and baseline (x-axis) residuals, with respect to 2 parameters: 1-norm and infinity-norm, visualized in 3D and 2D space

2.3. Statistical Properties of Wrong Fixings

At first, we would compute some general statistics such as the simulation-based success rate for fixing P_s for which **Q_GUI** only outputs the lower bound, the probability of good performance among all wrong fixings P_{sw} which is very important since we need to make sure this probability is larger than zero before validation. Besides, it is also necessary to compute probability based on (1.13), but we compute $P(\|\hat{\mathbf{b}}-\check{\mathbf{b}}\|^2_{\mathbf{Q}_{\hat{b}\hat{b}}} \leq \beta^2)$ together with other 2 probabilities $P(\|\check{\mathbf{b}}-\mathbf{b}\|^2_{\mathbf{Q}_{\check{b}\check{b}}} \leq \beta^2)$ and $P(\|\hat{\mathbf{b}}-\mathbf{b}\|^2_{\mathbf{Q}_{\hat{b}\hat{b}}} \leq \beta^2)$ with $\alpha_1 = P_s - 0.02$ in (1.13), to check if float and fixed solution are well bounded. The selection of this value of α_1 is aimed to make sure the computed probability corresponds well to the bound of residual of baseline parameters, since the bound of residual is related to the success rate.

Based on Section 2.2 we define 4 validation methods:

1. **Infinity-norm ratio detection (RD)** which is based on Figure 2.4, and here we use 3 different thresholds based on (2.6) for the ratio of infinity-norm between wrong baseline and ambiguity residuals;

$$\begin{aligned}
\mathbf{RD}_{threshold_1} &= \mathbf{mean}(ratio_{w,good}) + 1.96 \cdot \mathbf{std}(ratio_{w,good}) \\
\mathbf{RD}_{threshold_2} &= \mathbf{mean}(ratio_{w,good}) + \mathbf{std}(ratio_{w,good}) \\
\mathbf{RD}_{threshold_3} &= \mathbf{mean}(ratio_{w,good})
\end{aligned} \tag{2.6}$$

where $w, good$ represents good performance in wrong fixings.

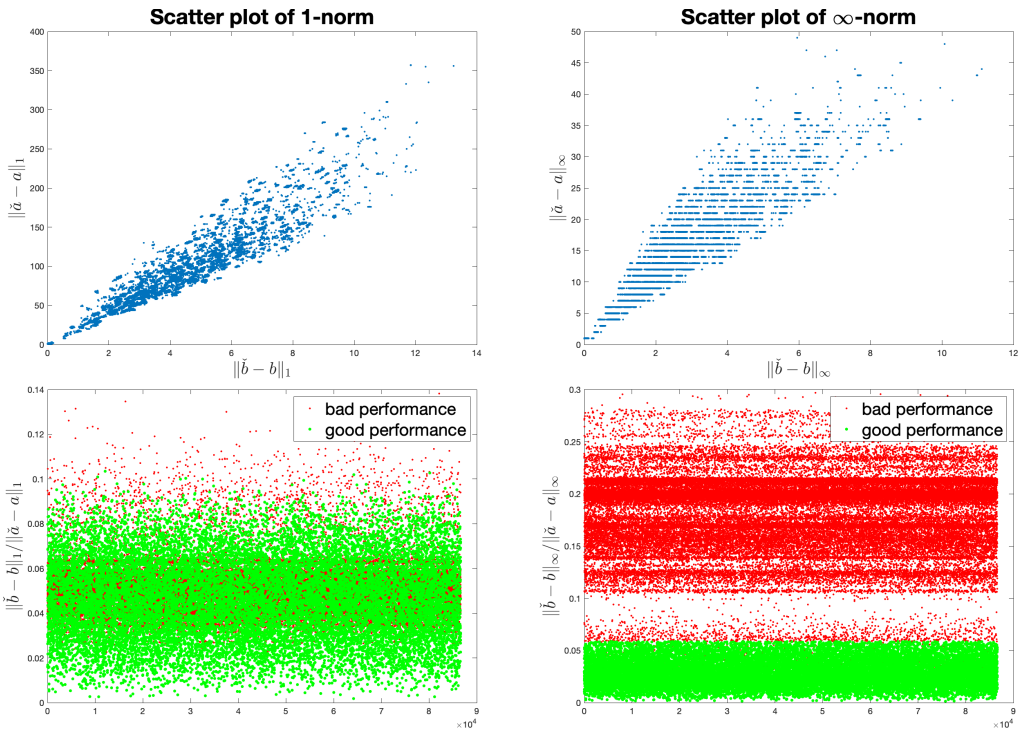

Figure 2.4: Top two are scatter plots of the 1-norm and infinity-norm of residuals for wrong ambiguity vs. baseline, and bottom two are sequences of corresponding ratios between wrong baseline and ambiguity residuals, separated by good performance (green dot) and bad performance (red dot)

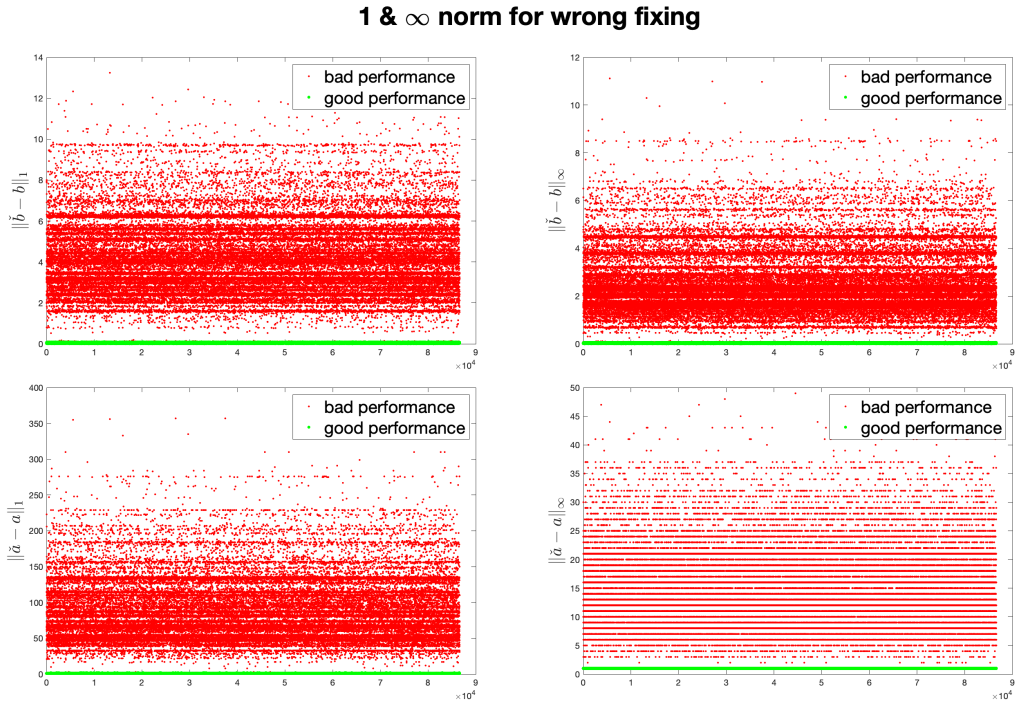

Figure 2.5: Sequences of 1-norm or infinity-norm for wrong baseline or ambiguity residuals, separated by good performance (green dot) and bad performance (red)

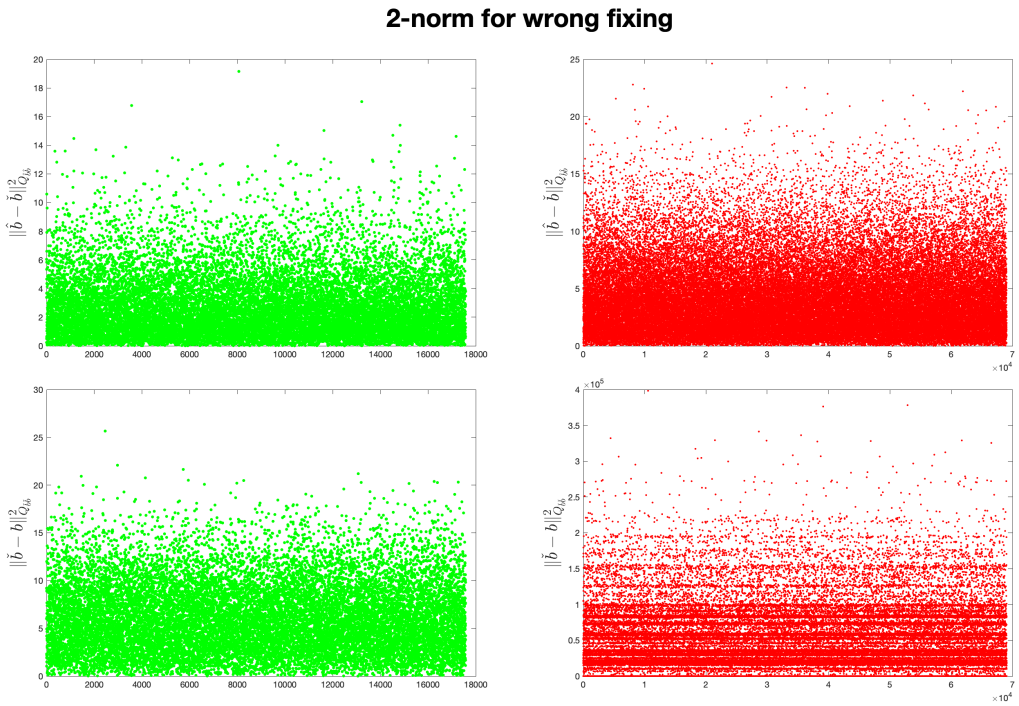

Figure 2.6: Sequences of weighted 2-norm for wrongly fixed baseline residuals and corresponding residuals of float solution, with good performance shown in green and bad performance shown in red

2. **Weighted 2-norm detection (WD)** which is based on Figure 2.6, and we retrieve a threshold based on (2.7) from correct fixing for the weighted 2-norm of the wrong fixing;

$$\mathbf{WD}_{threshold} = 0.95 \cdot \mathbf{max}(\|\check{\mathbf{b}} - \mathbf{b}\|^2_{\mathbf{Q}_{\check{\mathbf{b}}\check{\mathbf{b}},c}}) \tag{2.7}$$

where c represents correct fixing.

3. **1-norm baseline residual detection (BD1)** which is based on Figure 2.5, and we set a threshold from the range of the wrong fixing with good performance, for the 1-norm of wrong fixing residuals. It is hard to decide which value would be better, so it is better to use one based on (2.8) from the true value, and we will try to find a proper threshold in time series analysis;

$$\mathbf{BD1}_{threshold} = 0.95 \cdot \mathbf{max}(\|\check{\mathbf{b}} - \mathbf{b}\|_{1,w,good}) \tag{2.8}$$

4. **Infinity-norm baseline residual detection (BDi)** which is very similar to the previous method, but for the infinity-norm of wrong fixing residuals. Threshold is computed from (2.9)

$$\mathbf{BDi}_{threshold} = 0.95 \cdot \mathbf{max}(\|\check{\mathbf{b}} - \mathbf{b}\|_{\infty,w,good}) \tag{2.9}$$

In order to assess these four methods, we could compute four parameters for each:

1. **the rate of participation** P_{par} which describes among all wrong fixings with good performance, the percentage of those that could be detected;

2. **the success rate of detection** P_d which shows among all wrong fixings under the threshold, the percentage of those that are correctly detected as good performance;

3. **the rate of misdiagnose** P_m which describes among all wong fixings with bad performance, the percentage of those are incorrectly detected as good performance. It is also a significant parameter. If $P_{sw} = 0$, when other three parameters are meaningless since there is no wrong fixing with good performance, we could validate whether there are bad performances under the threshold we set;

	True good performance	True bad performance	
Predicted good performance	S_{gg}	S_{gb}	S_{accept}
Predicted bad performance	S_{bg}	S_{bb}	S_{reject}
	S_{good}	S_{bad}	

Table 2.1: Binary confusion table of true/predicted good/bad performance among wrong fixings

4. γ which is the ratio between P_m and $P_d \cdot P_{sw}$, a smaller γ means the detection performs well. Ideally, it should be equal to zero all the time. In a relatively ideal circumstance, with $P_m \leq 1\%$ and $P_d \geq 90\%$, γ should be less than or equal to $0.011/P_{sw}$ (we do not give a exact value for P_{sw} since it varies a lot over time in different scenarios).

Intuitively, P_{sw}, P_{par}, P_d and P_m could be shown as (2.10) with Table 2.1. More clearly, S means **set of wrong fixings** ($S = \{x \in all\ fix. | label(x) = wrong\ fix.\}$), for S_{gg}, S_{gb}, S_{bg}, S_{bb}, the first subscript represents predicted performance and the second represents true performance. $S_{good} = S_{gg} + S_{bg}$, $S_{bad} = S_{gb} + S_{bb}$, $S_{accept} = S_{gg} + S_{gb}$, $S_{reject} = S_{bg} + S_{bb}$. Besides, P_{par} describes the recall of the validation and P_d describes the precision of the validation. We do not compute the overall accuracy of the validation ($\frac{S_{gg}+S_{bb}}{S_{good}+S_{bad}}$) since S_{bb} usually has a much larger size than S_{gg}, and it would dominate the final result a lot. As a result, the accuracy would describe more about how many wrong fixings with bad performance are correctly rejected, which is unrelated to our research.

$$
\begin{aligned}
P_{sw} &= P(true\ good | wrong\ fix.) = \frac{S_{good}}{S_{good} + S_{bad}} = \frac{S_{good}}{S} \\
P_{par} &= P(predicted\ good\ \&\ true\ good | true\ good\ \&\ wrong\ fix.) = \frac{S_{gg}}{S_{good}} \\
P_d &= P(predicted\ good\ \&\ true\ good | predicted\ good\ \&\ wrong\ fix.) = \frac{S_{gg}}{S_{accept}} \\
P_m &= P(predicted\ good\ \&\ true\ bad | true\ bad\ \&\ wrong\ fix.) = \frac{S_{gb}}{S_{bad}}
\end{aligned}
\tag{2.10}
$$

Using thresholds from (2.6) to (2.9), together with other data, we not only output statistics for epoch 285 as Table 2.2 shows, but also another epoch in Table 2.3. From these two tables, we could see that the probability $P(\|\hat{\mathbf{b}} - \mathbf{b}\|^2_{\mathbf{Q}_{\hat{b}\hat{b}}} \leq \beta^2)$ and $P(\|\hat{\mathbf{b}} - \check{\mathbf{b}}\|^2_{\mathbf{Q}_{\hat{b}\hat{b}}} \leq \beta^2)$ are always well bounded, while the probability of $P(\|\check{\mathbf{b}} - \mathbf{b}\|^2_{\mathbf{Q}_{\check{b}\check{b}}} \leq \beta^2)$ is affected by the success rate P_s obviously. P_{sw} is very random and if it is larger than 0 we could apply our validation method. As for the detection result, obviously a smaller threshold value would lead to a higher P_d and a lower chance of misdiagnose, based on results form **RD** method, while at the same time less fixings are enrolled and P_{par} decreases sharply. In practice, we would prioritize the success rate if P_{par} is not very low. P_m shows if our validation is always reliable especially for the case $P_{sw} = 0$. In our two cases it is always smaller than 4%, which means our methods work well currently, under the circumstance where there exist fixings with good performance. And γ could help us compare the performance of different methods. If the success rates P_d are the same for two methods, we would consider the one with smaller rate of misdiagnose P_m, meaning the one with a smaller γ. Here P_{sw} could be considered as a scaling factor to make the value of γ to a proper range over time series, to enable us to clearly check in which epochs the method works well.

We could not draw a conclusion from these two tables that which method would be proper for the validation. While **BDi** is likely to get a close result as **RD** under similar threshold since the baseline residual is small when the ambiguity residual is not large in general, based on Figure 2.4, which means that if a wrong fixing has good performance, $\|\check{\mathbf{a}} - \mathbf{a}\|_\infty$ is more likely to be equal to 1. And all of these four methods are reliable so far.

Finally, we visualize the distribution of some statistics, shown as Figure 2.7 and 2.8. And the first figure we see a χ^2 distribution for 2-norm and normal distribution in horizontal successful fixings, while no information of regular distribution could be retrieved from histogram of the wrong fixing. In terms of the second figure, for the histogram of all fixings, it shows in fact there are less wrong fixings especially in the further area, although we have observed a lot of clusters in Figure 2.2, which is a bit tricky. And the distribution of wrong ambiguity residual is a bit similar to horizontal residual, which might be explained by (1.4) and (1.5).

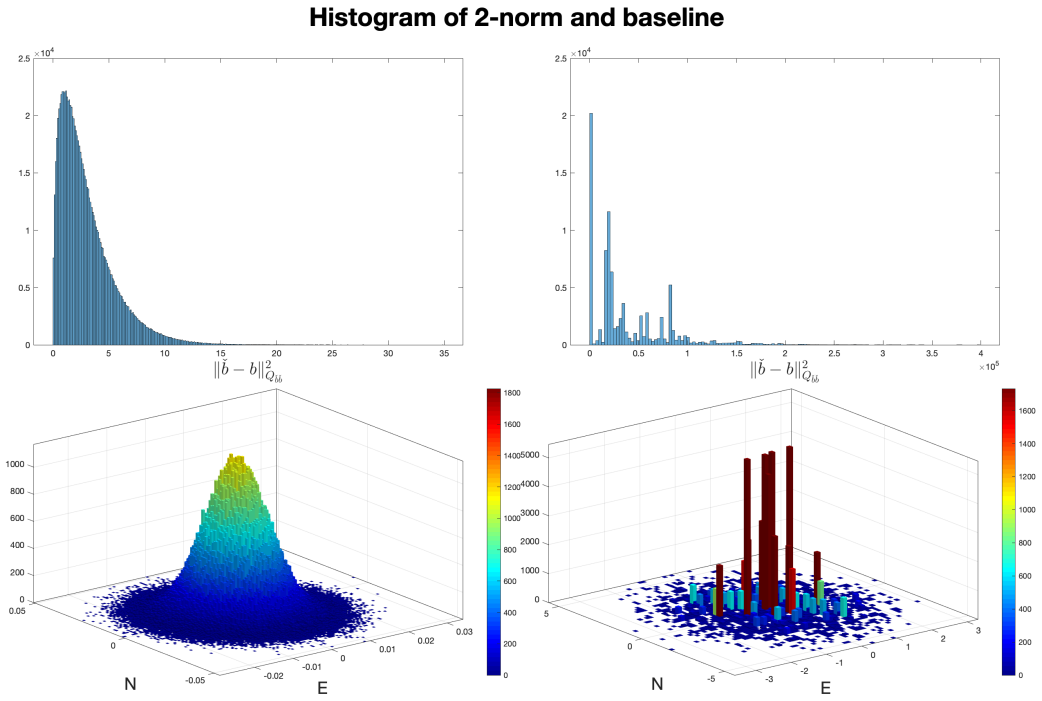

Figure 2.7: Histogram of correctly (bottom left) and wrongly (bottom right) fixed horizontal residual, together with corresponding histogram of weighted 2-norm (top two)

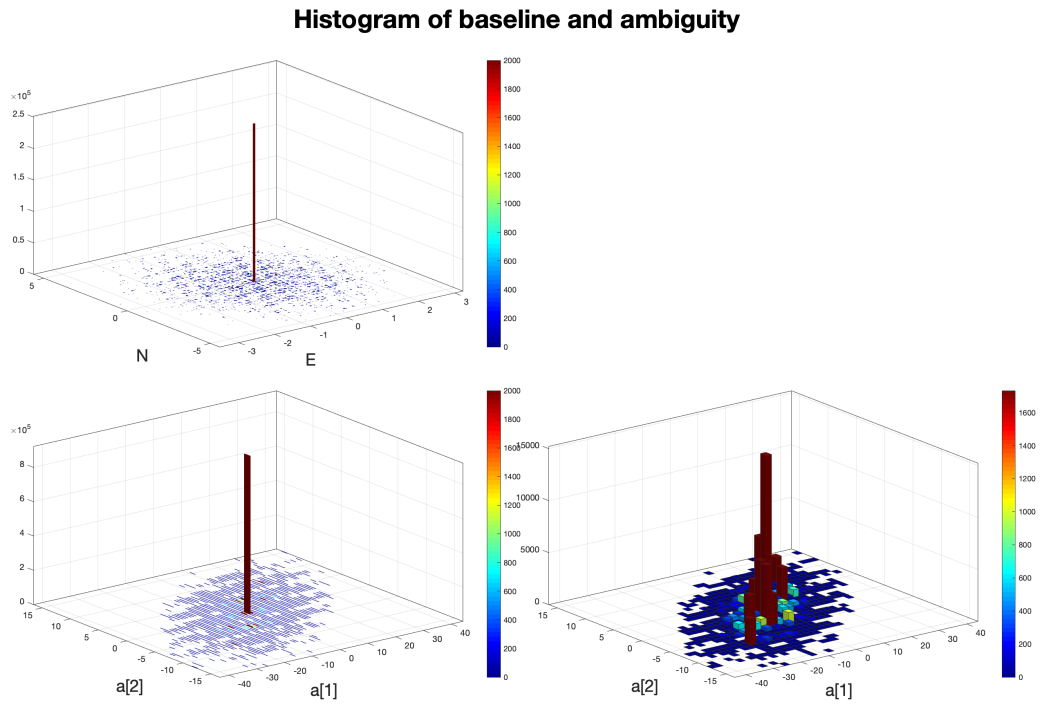

Figure 2.8: Histogram of all fixed horizontal residual (top left), together with the first and second ambiguity residual (bottom left: all fixings; bottom right: wrong fixings)

Epoch	P_s	P_{sw}	$P(\|\check{\mathbf{b}}-\mathbf{b}\|^2_{\mathbf{Q}_{\check{b}\check{b}}} \le \beta^2)$	$P(\|\hat{\mathbf{b}}-\mathbf{b}\|^2_{\mathbf{Q}_{\hat{b}\hat{b}}} \le \beta^2)$	$P(\|\hat{\mathbf{b}}-\check{\mathbf{b}}\|^2_{\mathbf{Q}_{\hat{b}\hat{b}}} \le \beta^2)$
285	91.34%	20.29%	90.78%	97.80%	98.10%
Method	Threshold	P_{par}	P_d	P_m	$\gamma = P_m/(P_d P_{sw})$
RD	0.05	96.56%	93.31%	1.76%	0.09
	0.04	81.33%	93.96%	1.33%	0.07
	0.03	54.21%	98.95%	0.15%	0.01
WD	33.12	100.00%	87.66%	3.58%	0.20
BD1	0.10	99.94%	89.28%	3.05%	0.17
BDi	0.06	97.78%	93.30%	1.79%	0.09

Table 2.2: Some statistics for validation in epoch 285

Epoch	P_s	P_{sw}	$P(\|\check{\mathbf{b}}-\mathbf{b}\|^2_{\mathbf{Q}_{\check{b}\check{b}}} \le \beta^2)$	$P(\|\hat{\mathbf{b}}-\mathbf{b}\|^2_{\mathbf{Q}_{\hat{b}\hat{b}}} \le \beta^2)$	$P(\|\hat{\mathbf{b}}-\check{\mathbf{b}}\|^2_{\mathbf{Q}_{\hat{b}\hat{b}}} \le \beta^2)$
1	81.12%	2.85%	79.53%	97.54%	98.48%
Method	Threshold	P_{par}	P_d	P_m	$\gamma = P_m/(P_d P_{sw})$
RD	0.05	97.14%	86.87%	0.43%	0.17
	0.04	83.01%	92.21%	0.20%	0.08
	0.03	50.64%	98.77%	0.02%	0.01
WD	30.77	100.00%	79.34%	0.76%	0.34
BD1	0.10	99.96%	82.12%	0.64%	0.27
BDi	0.05	97.43%	86.84%	0.43%	0.17

Table 2.3: Some statistics for validation in epoch 1

2.4. Time Series Analysis

Furthermore, it is necessary to visualize these statistics above in time series, to check if our method could be generally applied under different circumstances during a whole day as well as some changes over time.

At first we plot some figures for the scenario we mentioned above with 10^4 samples for efficiency for each epoch, shown as Figure 2.9 to 2.14:

In this scenario, the success rate of fixing varies with the number of satellites, and especially it is very high when the number of satellites is over ten. And there is an obvious decrease for the standard deviation when P_s is high enough since a high success rate for fixing means more samples are applied for the estimation, leading to a more precise result. And the worst standard deviation could be two times as the best. The baseline fixing is more precise in east and less in up in general. The horizontal correlation also fluctuates. Besides, It is interesting to see that when $P_s \ge 90\%$, P_{sw} would not be close to zero, but there is also an anomaly that P_{sw} is very high between about epoch 230 to 280, when P_s is almost one. This anomaly might be out of accident since if $P_s = 99\%$, there would be only $10^4 \times 1\% = 100$ wrong fixing samples and 10 for $P_s = 99.9\%$ whose size is very small. And the number would be even smaller if we set a threshold. Figure 2.10 shows both float and fixing errors are well bounded if P_s is high, and $P(\|\hat{\mathbf{b}}-\check{\mathbf{b}}\|^2_{\mathbf{Q}_{\hat{b}\hat{b}}} \le \beta^2)$ shows a contrary trend comparing with other two probabilities, but all of them seem to converge to a certain constant if P_s is good enough.

In terms of those four detection methods we mentioned, we set a loose and a tight threshold which is constant over time as Figure 2.11 to 2.14 show. Obviously a tight threshold could improve the performance of detection, while P_{par} would decrease a lot. For each time series, we could always observe drops of P_d in some epochs, and this is due to that in most epochs P_{sw} is very low, and after we set a threshold only a few samples are enrolled to compute statistics, leading to a more random result possibly. While we could confirm it by P_m, and although it also shows an anomaly between epoch 230 to 280, before that it is very close to zero, which means that below the threshold the size of wrong fixings with bad performance is also very small. We could only get an overall view from plots of time series based on 10^4 sample size, that the success rate of the detection method is above 80% in most time under loose threshold and it would be very reliable with tight threshold. In terms of the anomaly between epoch 230 to 280, when P_m and γ are very large sometimes, we also increase the sample to 5×10^4 and there are some decreases, but not obviously. So we choose one epoch to visualize the detail to see whether the anomaly is true or not.

Noticing that $P_m = 1$ in epoch 238, we compute the same statistics as Table 2.2 and 2.3, shown as Table 2.4. It shows that based on a large sample size, the result is much better and P_m is much smaller than 1 although it is larger than the result in epoch 1 and 285. Besides, we could see there is a obvious decrease of P_m if we

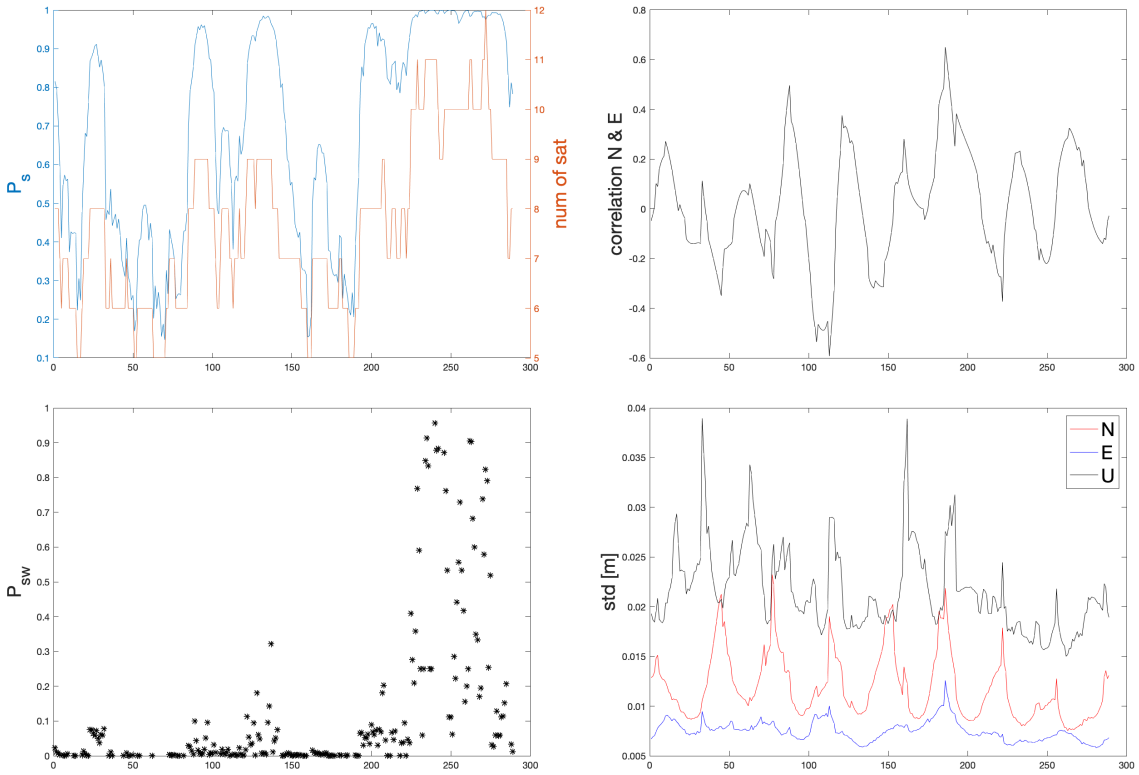

Figure 2.9: Time series of P_s, P_{sw}, number of satellites, horizontal correlation and standard deviation in N, E & U

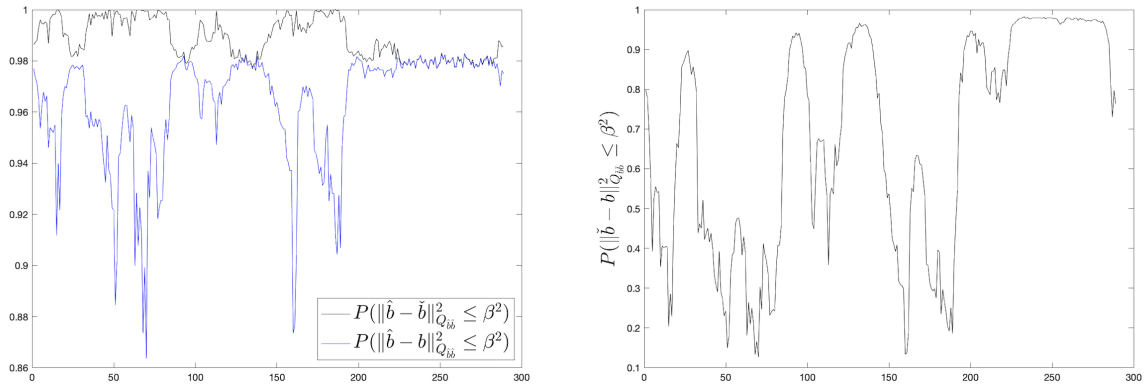

Figure 2.10: Time series of $P(\|\check{\mathbf{b}}-\mathbf{b}\|^2_{\mathbf{Q}_{\check{\mathbf{b}}\check{\mathbf{b}}}} \leq \beta^2)$ $P(\|\hat{\mathbf{b}}-\mathbf{b}\|^2_{\mathbf{Q}_{\hat{\mathbf{b}}\hat{\mathbf{b}}}} \leq \beta^2)$ and $P(\|\hat{\mathbf{b}}-\check{\mathbf{b}}\|^2_{\mathbf{Q}_{\hat{\mathbf{b}}\hat{\mathbf{b}}}} \leq \beta^2)$

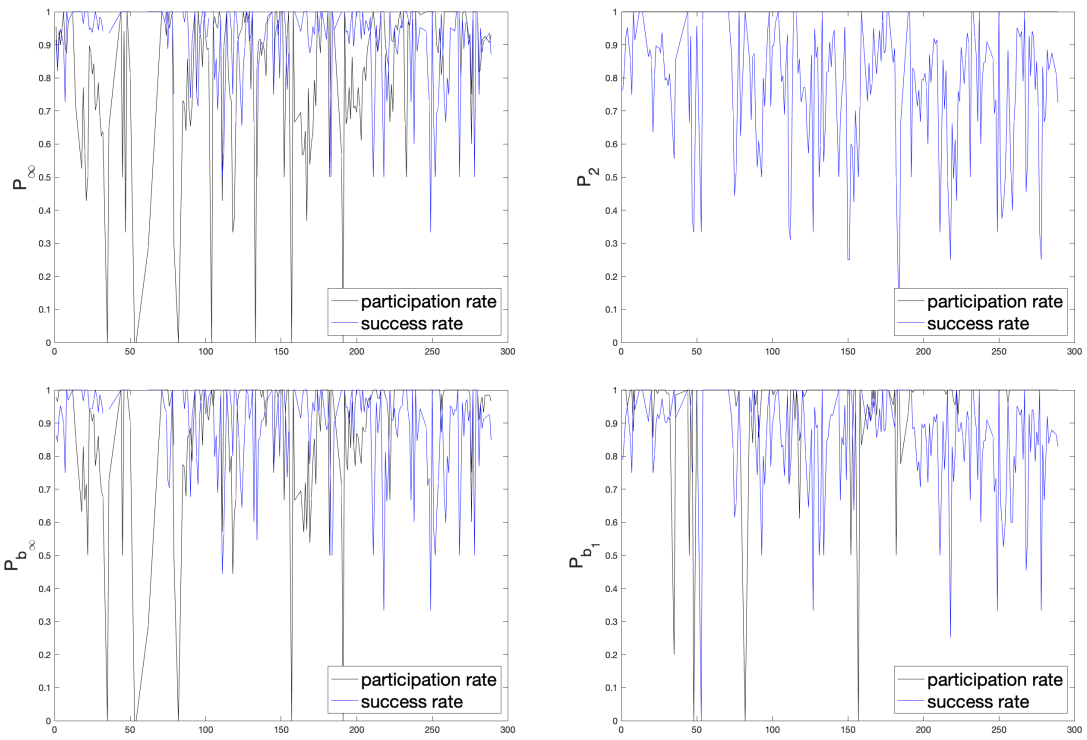

Figure 2.11: Time series of P_d (success rate), P_{par} (participation rate) for **RD** (P_∞), **WD** (P_2), **BDi** (P_{b_∞}) and **BD1** (P_{b_1}) under loose thresholds

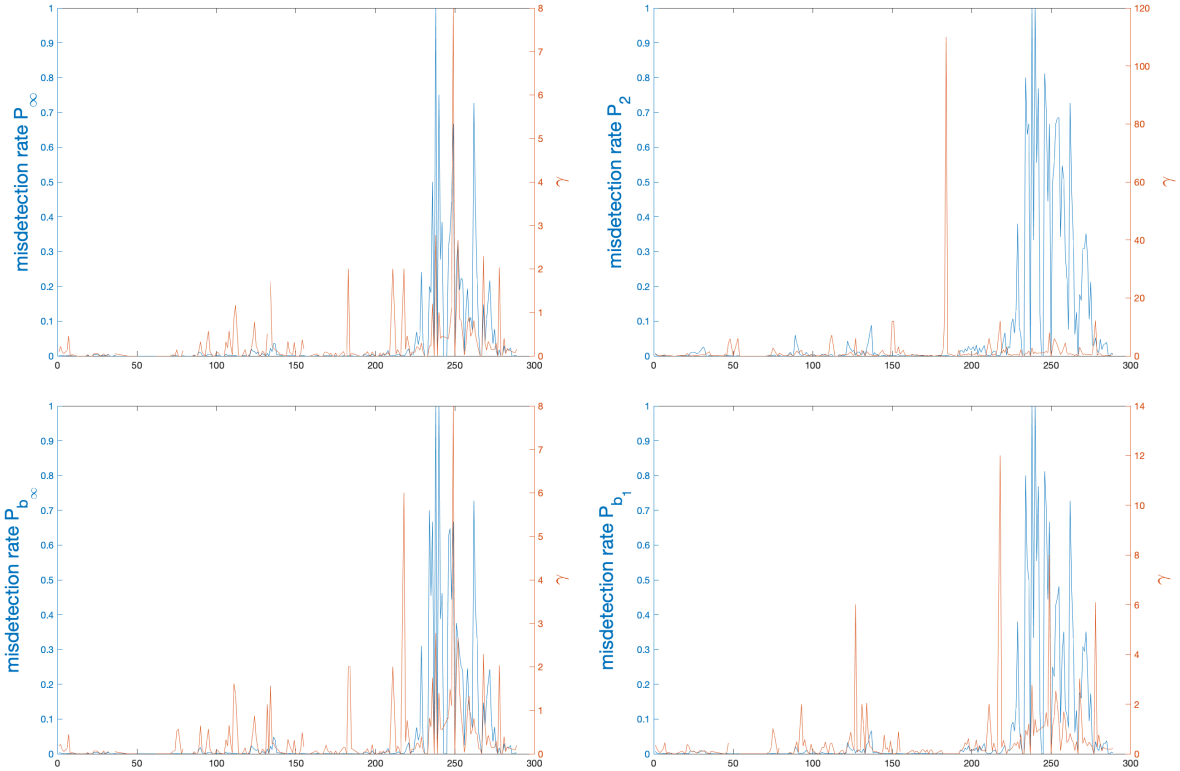

Figure 2.12: Time series of P_m (misdetection rate), γ for **RD** (P_∞), **WD** (P_2), **BDi** (P_{b_∞}) and **BD1** (P_{b_1}) under loose thresholds

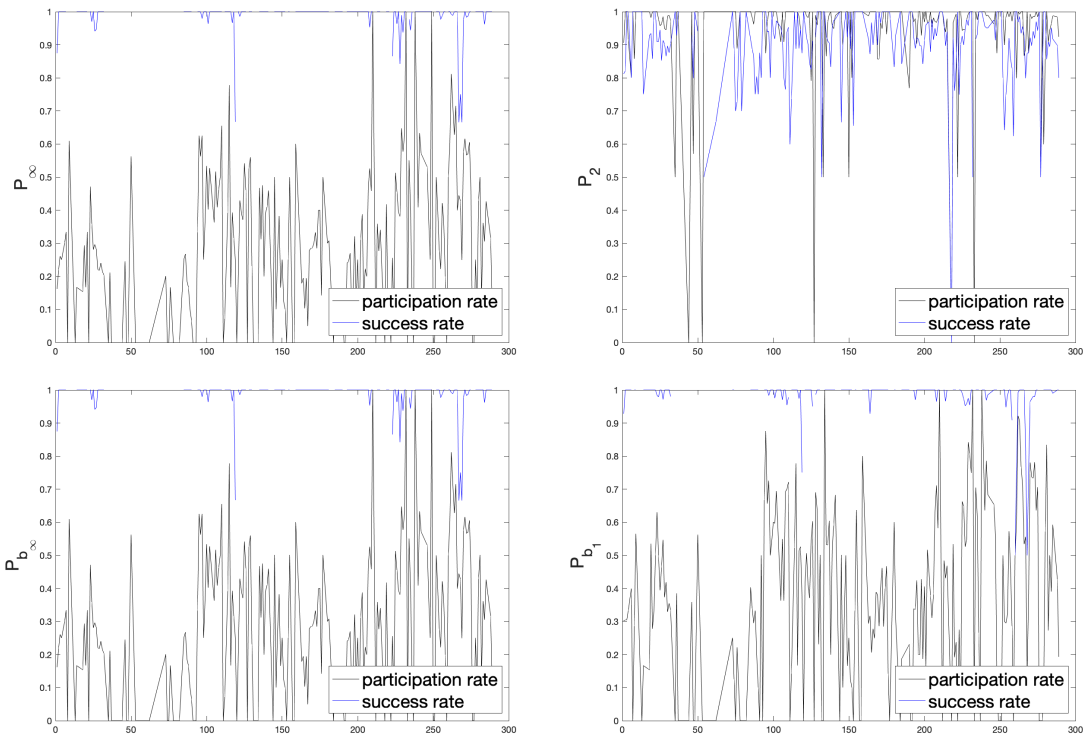

Figure 2.13: Time series of P_d (success rate), P_{par} (participation rate) for **RD** (P_∞), **WD** (P_2), **BDi** (P_{b_∞}) and **BD1** (P_{b_1}) under tight thresholds

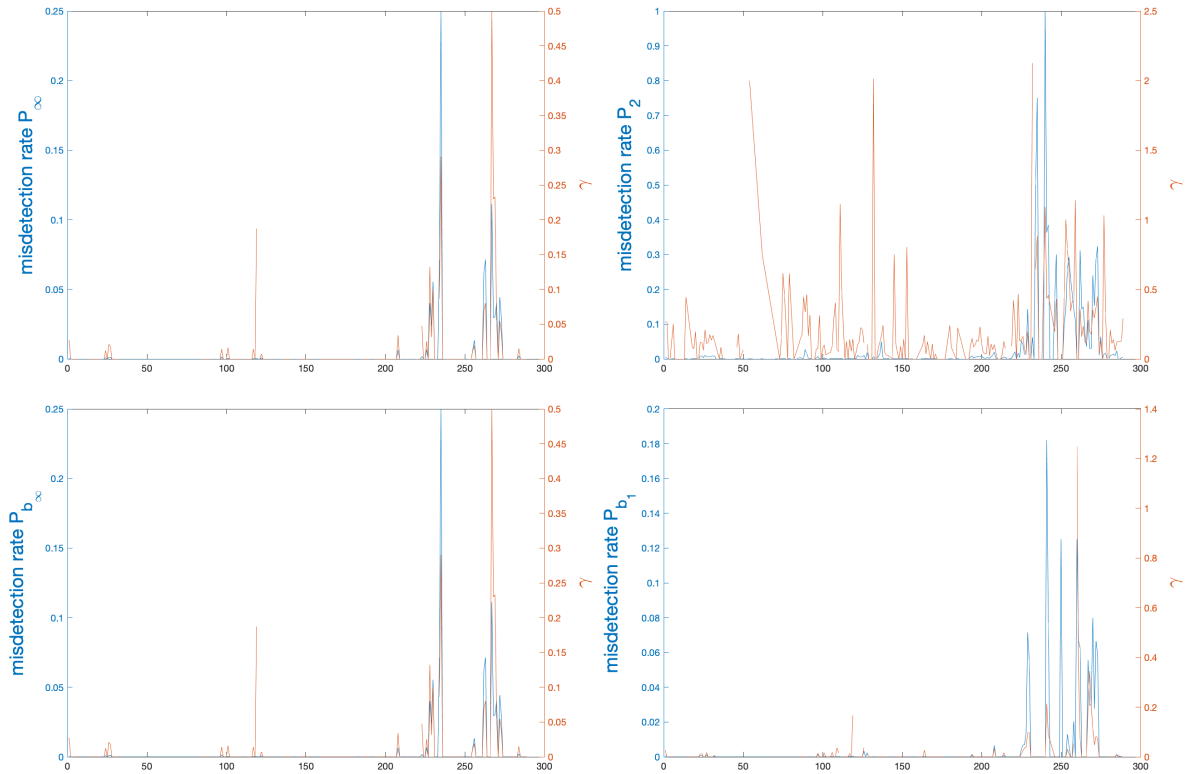

Figure 2.14: Time series of P_m (misdetection rate), γ for **RD** (P_∞), **WD** (P_2), **BDi** (P_{b_∞}) and **BD1** (P_{b_1}) under tight thresholds

use a tight threshold based on method **RD**. The last plot in Figure 2.15 gives the detail for the method **RD**, and there are not many wrong fixings, about $10^6 \times 0.0446\% = 446$ samples, but we could figure out a general trend from the plot. One possibility leading to the deep overlap between good and bad performance is that the success rate for fixing is very high, and as a result, some wrong fixings are just a bit larger than the 3σ interval and labeled as bad performance. So it really depends to find a proper threshold in different epochs and circumstances, and sometimes we might also give a larger confidence interval to define good performance, when P_s is very high.

Epoch	P_s	P_{sw}	$P(\|\check{\mathbf{b}}-\mathbf{b}\|^2_{\mathbf{Q}_{\check{b}\check{b}}} \le \beta^2)$	$P(\|\hat{\mathbf{b}}-\mathbf{b}\|^2_{\mathbf{Q}_{\hat{b}\hat{b}}} \le \beta^2)$	$P(\|\hat{\mathbf{b}}-\check{\mathbf{b}}\|^2_{\mathbf{Q}_{\hat{b}\hat{b}}} \le \beta^2)$
238	99.96%	28.03%	97.95%	98.02%	98.02%
Method	Threshold	P_{par}	P_d	P_m	$\gamma = P_m/(P_d P_{sw})$
RD	0.05	100.00%	66.49%	19.63%	1.05
	0.04	80.00%	70.42%	13.08%	0.66
	0.03	55.20%	79.31%	5.61%	0.25
WD	27.04	100.00%	54.58%	32.40%	2.12
BD1	0.08	99.20%	68.13%	18.07%	0.95
BDi	0.05	92.80%	67.44%	17.44%	0.92

Table 2.4: Some statistics for validation in epoch 238

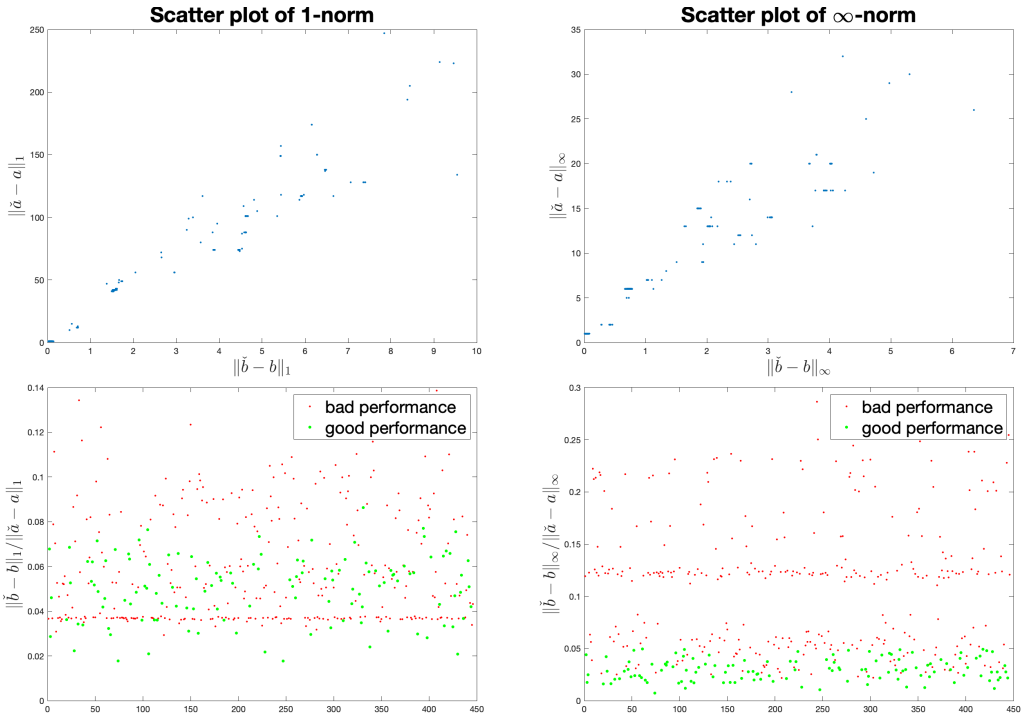

Figure 2.15: Top two are scatter plots of the 1-norm and infinity-norm of residuals for wrong ambiguity vs. baseline, and bottom two are sequences of corresponding ratios between wrong baseline and ambiguity residuals, separated by good performance (green dot) and bad performance (red dot)

In terms of the scenario of single frequency (L1 only), we decrease the standard deviation of code to 20 cm and phase to 2 mm, based on Figure 2.1, to generate a time series as well, together with time series based on the same circumstance but with dual-frequency (L1+L5) as a contrast, shown as Figure 2.16 and 2.17. These two figures show a smaller standard deviation in horizontal and vertical because of more precise phase and code measurements. One interesting thing is that both scenarios do not detect good performances among wrong fixings, for single frequency it means the **LAMBDA** method operates well, and for dual-frequency, it is due to the high success rate under less noise of code and phase measurement. Both scenarios have a zero P_m so no bad performance is incorrectly detected.

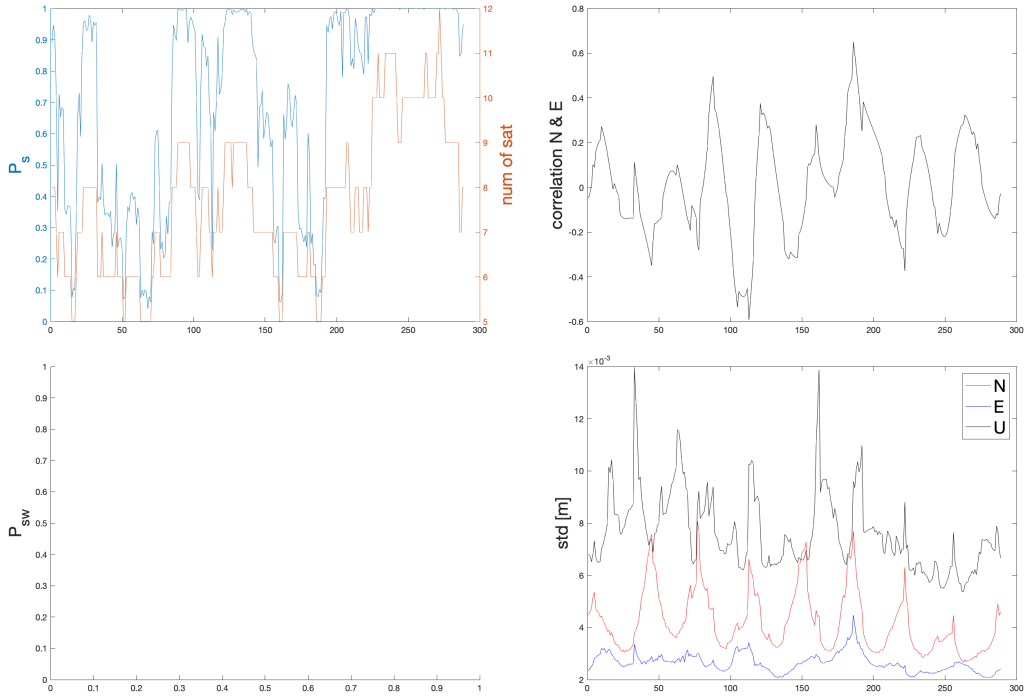

Figure 2.16: Time series of P_s, P_{sw}, number of satellites, horizontal correlation and standard deviation in N, E & U for single frequency with small standard deviation

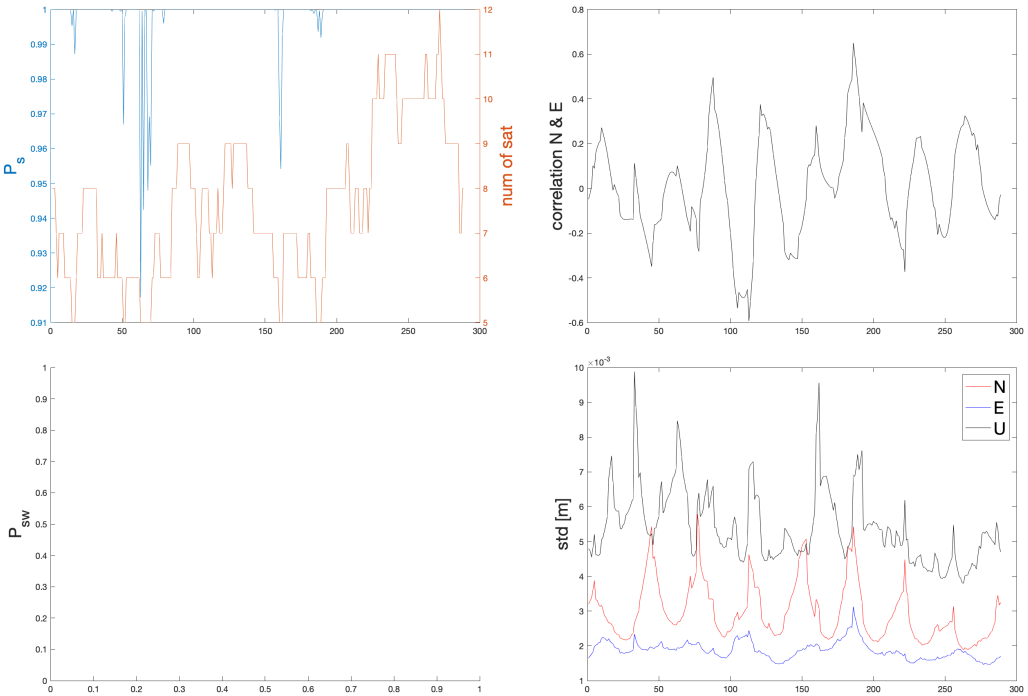

Figure 2.17: Time series of P_s, P_{sw}, number of satellites, horizontal correlation and standard deviation in N, E & U for dual frequencies with small standard deviation

In a word, although the visualization in time series is not as precise as that for single epoch, we could induce that we could detect the good performance among wrong fixings, but need to take a more adaptive method to find a proper threshold and sometimes we could also take a partial threshold to include some fixings that are labeled as bad performance. It is a bit complicated indeed, so we want to apply some methods, like a filter, to make sure after some epochs, the result is so reliable that we need not to do the detection.

3

Improvement of Kalman Filter (KF)

We have analysed the performance of wrong fixings estimated from each epoch, now we could apply a filter, and Kalman filter is a efficient way to improve the precision of estimation over time since it is a recursive estimator and the estimation in previous time step could be used as the initial state in the next time step, and the current measurement could be used as correction to lessen the standard deviation of estimated parameters. In addition to the improvement of fixing success rate and horizontal standard deviations, we would care about how wrong fixings could perform during the processing.

3.1. Multi-epoch LSE

Multi-epoch **LSE** is a simple method to improve the precision of the estimation, although more time-consuming:

$$\mathbf{Q}_{multi} = \frac{1}{K}\mathbf{Q} \tag{3.1}$$

with K the number of epochs we combine and during these K epochs the circumstance would be in constant.

We could apply a 10-epoch **LSE** for the scenario of single frequency in section 2.2 when P_s is always very low, to see the improvement, shown as Figure 3.1 and 3.2. We could also compute the standard deviations for the result applying normal **LSE** by (3.2):

$$\sigma_{\mathbf{LSE}} = \sqrt{K}\sigma_{K-epoch\,\mathbf{LSE}} \tag{3.2}$$

Although it is a bit time consuming, multi-epoch **LSE** is a effective way to improve the success rate for fixing as well as precision of baseline, and easy to implement. While sometimes we cannot make sure a long time stable circumstance, especially for a dynamic scenario where the environment is changing all the time. In this case we cannot apply the multi-epoch **LSE** any more, but use a filter.

3.2. Basic Model of Kalman Filter for GNSS

For a static scenario, a simple model of Kalman filter in our **DD** case could be shown as:

$$\begin{bmatrix}\mathbf{b}\\ \mathbf{a}\end{bmatrix}_{k+1} = \begin{bmatrix}\mathbf{b}\\ \mathbf{a}\end{bmatrix}_{k} + \begin{bmatrix}\Delta\mathbf{t}\\ \mathbf{0}\end{bmatrix} w_k \tag{3.3}$$

$$\mathbf{P}_{k+1|k} = \mathbf{P}_k + \mathbf{S}_k \tag{3.4}$$

where $\mathbf{S}_k = \mathbf{B}\mathbf{Q}_k\mathbf{B}^{\mathrm{T}}$ with $\mathbf{Q}_k = \sigma^2_{w_k} = 10^{-4}[m^2]$, w_k noise and $\mathbf{B} = [\Delta\mathbf{t} \quad 0]^{\mathrm{T}}$, Δt the time interval [s], $\mathbf{P}_k$ is variance-covariance matrix at epoch k;

$$\mathbf{K}_{k+1} = \mathbf{P}_{k+1|k}\mathbf{A}^{\mathrm{T}}_{k+1}(\mathbf{R_{k+1}} + \mathbf{A}_{k+1}\mathbf{P}_{k+1|k}\mathbf{A}^{\mathrm{T}}_{k+1})^{-1} \tag{3.5}$$

with $\mathbf{A}_{k+1}$ the design matrix at epoch $k+1$, $\mathbf{R}_{k+1}$ the variance-covariance matrix of measurement, given by (2.3);

$$\mathbf{P}_{k+1} = (\mathbf{I} - \mathbf{K}_{k+1}\mathbf{A}_{k+1})\mathbf{P}_{k+1|k} \tag{3.6}$$

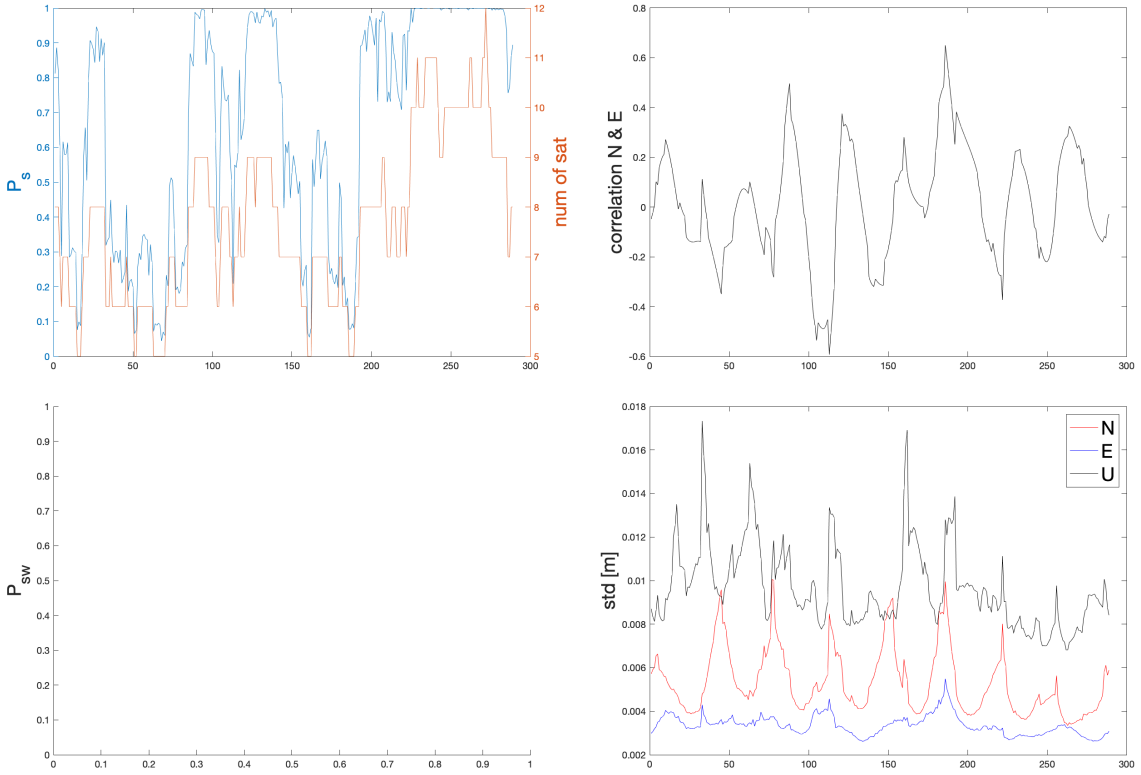

Figure 3.1: Time series of P_s, P_{sw}, number of satellites, horizontal correlation and standard deviation in N, E & U for single frequency

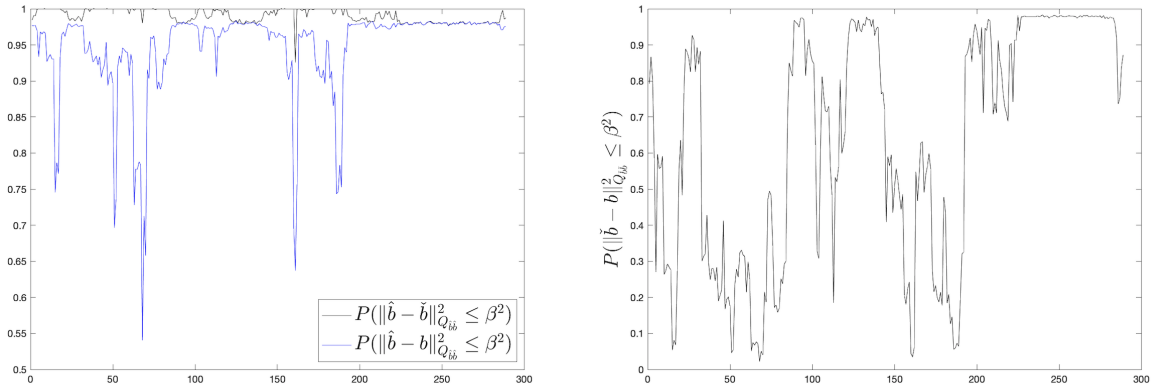

Figure 3.2: Time series of $P(\|\check{\mathbf{b}}-\mathbf{b}\|^2_{\mathbf{Q}_{\check{\mathbf{b}}\check{\mathbf{b}}}} \leq \beta^2)$ $P(\|\hat{\mathbf{b}}-\mathbf{b}\|^2_{\mathbf{Q}_{\hat{\mathbf{b}}\hat{\mathbf{b}}}} \leq \beta^2)$ and $P(\|\hat{\mathbf{b}}-\check{\mathbf{b}}\|^2_{\mathbf{Q}_{\hat{\mathbf{b}}\hat{\mathbf{b}}}} \leq \beta^2)$

Based on (3.3) to (3.6), we could update our variance-covariance matrix over time, by giving the initial state.

While in practice, during a day the number of satellites and the reference satellite would change sometimes. So $\mathbf{a}_k$ is not always the same. We could apply a transformation matrix based on the relationship between **DD** ambiguities with different reference satellite:

$$a_{mn,t} = a_{mx,t} - a_{nx,t} \tag{3.7}$$

with n the new reference satellite at epoch $t+1$ and x the previous reference satellite at epoch t, for any satellite m. And if m is a new satellite that has never appeared before, we need to initialize the variance with a relatively large value, such as $10 \cdot \mathbf{Q}_{\hat{\mathbf{a}}\hat{\mathbf{a}},\mathbf{LSE}}$.

So before the time step of Kalman filter, we should check if we need to do the transformantion or reinitialize part of the variance-covariance matrix, shown as (3.8) to (3.9):

$$\begin{bmatrix} \mathbf{Q}_{\hat{\mathbf{b}}\hat{\mathbf{b}}} & \mathbf{Q}_{\hat{\mathbf{b}}\hat{\mathbf{a}}} \\ \mathbf{Q}_{\hat{\mathbf{a}}\hat{\mathbf{b}}} & \mathbf{Q}_{\hat{\mathbf{a}}\hat{\mathbf{a}}} \end{bmatrix}^*_{n,t} = \begin{bmatrix} \mathbf{Q}_{\hat{\mathbf{b}}\hat{\mathbf{b}}} & \mathbf{Q}_{\hat{\mathbf{b}}\hat{\mathbf{a}}}\mathbf{T}' \\ \mathbf{T}\mathbf{Q}_{\hat{\mathbf{a}}\hat{\mathbf{b}}} & \mathbf{T}\mathbf{Q}_{\hat{\mathbf{a}}\hat{\mathbf{a}}}\mathbf{T}' \end{bmatrix}_{x,t} \tag{3.8}$$

$$\begin{bmatrix} \mathbf{Q}_{\hat{\mathbf{b}}\hat{\mathbf{b}}} & \mathbf{Q}_{\hat{\mathbf{b}}\hat{\mathbf{a}}} \\ \mathbf{Q}_{\hat{\mathbf{a}}\hat{\mathbf{b}}} & \mathbf{Q}_{\hat{\mathbf{a}}\hat{\mathbf{a}}} \end{bmatrix}_{n,t} = C\left(\begin{bmatrix} \mathbf{Q}_{\hat{\mathbf{b}}\hat{\mathbf{b}}} & \mathbf{Q}_{\hat{\mathbf{b}}\hat{\mathbf{a}}} \\ \mathbf{Q}_{\hat{\mathbf{a}}\hat{\mathbf{b}}} & \mathbf{Q}_{\hat{\mathbf{a}}\hat{\mathbf{a}}} \end{bmatrix}^*_{n,t} \right) \tag{3.9}$$

with transformation matrix $\mathbf{T}$ based on (3.7), and $C(\mathbf{X})$ the selection and reinitialization function which could select information that could be applied in epoch $t+1$ and set a variance $10 \cdot \mathbf{Q}_{\hat{\mathbf{a}}\hat{\mathbf{a}},\mathbf{LSE}}$ for new observation. And we assume zero correlations between new observation with other ambiguities as well as baseline parameters.

3.3. Visualization for Chosen Epochs

We randomly choose some epochs in scenario of both dual and single frequency to start filtering, by giving $P_0 = 10 \cdot \mathbf{Q}_{\mathbf{LSE},t}$ as initial condition at epoch t. We would only show the result for one starting epoch based on scenario of single frequency because for dual frequency it converges so fast that after 5 epochs (15 seconds each) there would not be any wrong fixing. Visualization of horizontal residuals starting from epoch 186 could be shown as Figure 3.3. We could observe a great improvement over time, and the success rate P_s for these 4 epochs are 0.1173%, 3.0752%, 61.1736%, 99.2488%, respectively. It is interesting that $P_{sw} = 0$ and $P_m = 0$ for all epochs under loose threshold, similar to the previous result of single frequency, which could be intuitively shown as Figure 3.4 and 3.5. For **RD** method, the ratio is always larger than 0.5, and 1-norm of baseline residual 0.5 and infinity-norm 0.2.

So far, Kalman filter is a reliable method in our scenario and furthermore we need to check the condition when the reference satellite or number of satellite change.

3.4. Time Series Analysis

As for the time series, we choose a 100-epoch length of Kalman filter processing for both dual and single frequency, starting from epoch 1 and 282, respectively, shown from Figure 3.6 to 3.9. $P_{sw} = 0$ for plots of single frequency and at the beginning of the scenario of dual frequencies, $P_{sw} > 0$ in some epochs, and it equals to zero after the success rate is very high. In terms of the anomaly in epoch 86 and 87, it could be considered as outlier, or they could also be labeled as correct fixing since P_s is very close to 1. The correlation plot shows a increase or decrease trend. And particularly, there is a small drop of success rate in Figure 3.8, about 1.5%, but P_s goes back to 1 quickly, meaning that the Kalman filter is very reliable. In terms of the standard deviation of baseline, error in north or up direction improves a lot, while in the east the standard deviation is very stable. In addition, in epoch 60 there is a jump for all of those three standard deviations due to the decrease of number of satellite shown in Figure 3.8.

Another interesting thing could be detected from Figure 3.9 and 3.10. During the first 100 steps we observe a increase of $P(\|\hat{\mathbf{b}} - \check{\mathbf{b}}\|^2_{\mathbf{Q}_{\hat{\mathbf{b}}\hat{\mathbf{b}}}} \leq \beta^2)$ after timestep 50 and other two probabilities are stable and are likely to converge to a certain value though with fluctuations. Furthermore, we visualize 100 extra timesteps for these three probabilities and the trend is the same as before. So it means there is a trend that the float solution is more likely to move towards the fixed solution, which is also shown as Figure 3.3, that the grey area gets smaller over time. As a result, after long enough time, the confidence level of the float solution could be the same as fixed solution.

In summary, Kalman filter is a reliable method to increase the success rate of fixing as well as the precision of positioning result. The residual is well bounded and converges very fast, and the confidence level of float

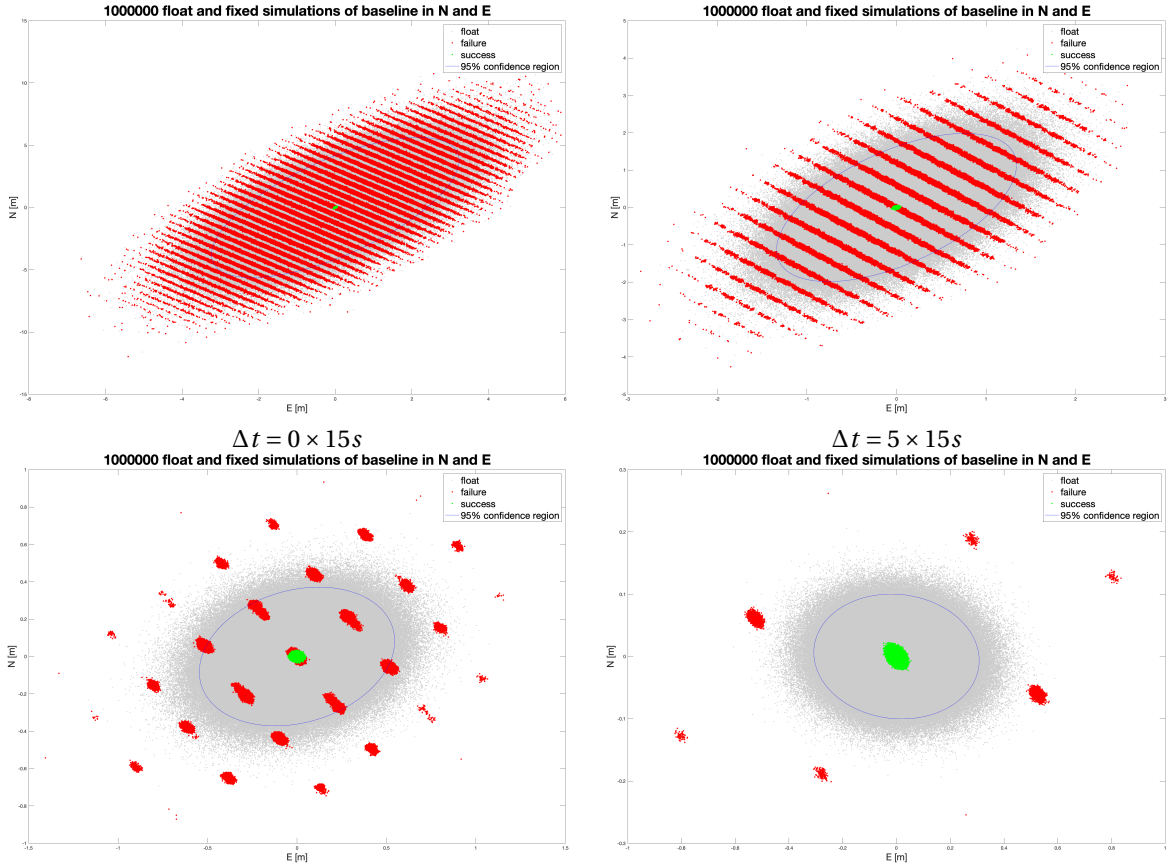

Figure 3.3: Horizontal residuals in 4 different timesteps during Kalman filter starting from epoch 186

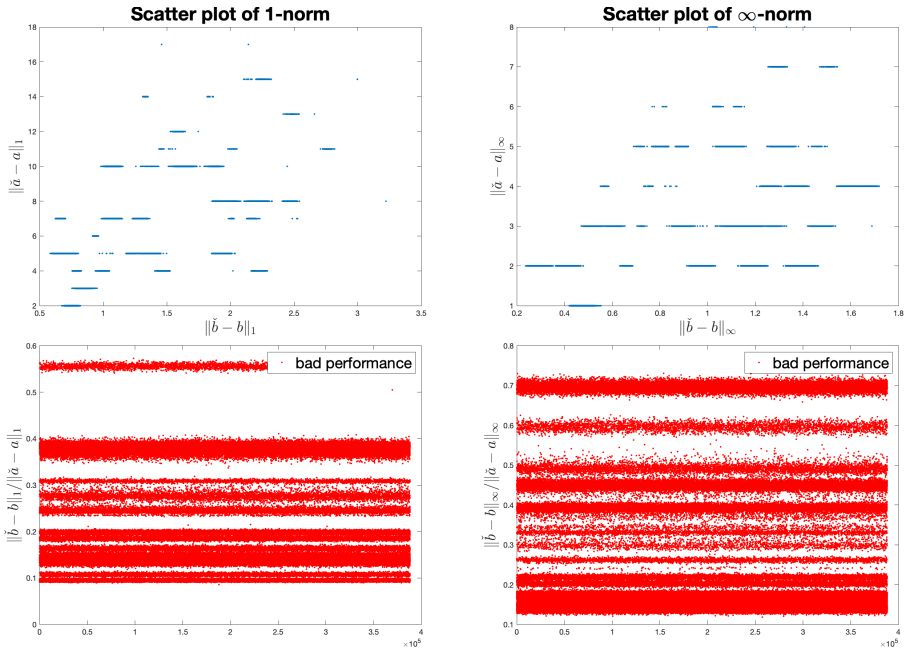

Figure 3.4: Top two are scatter plots of the 1-norm and infinity-norm of residuals for wrong ambiguity vs. baseline, and bottom two are sequences of corresponding ratios between wrong baseline and ambiguity residuals, separated by good performance (greed dot) and bad performance (red dot)

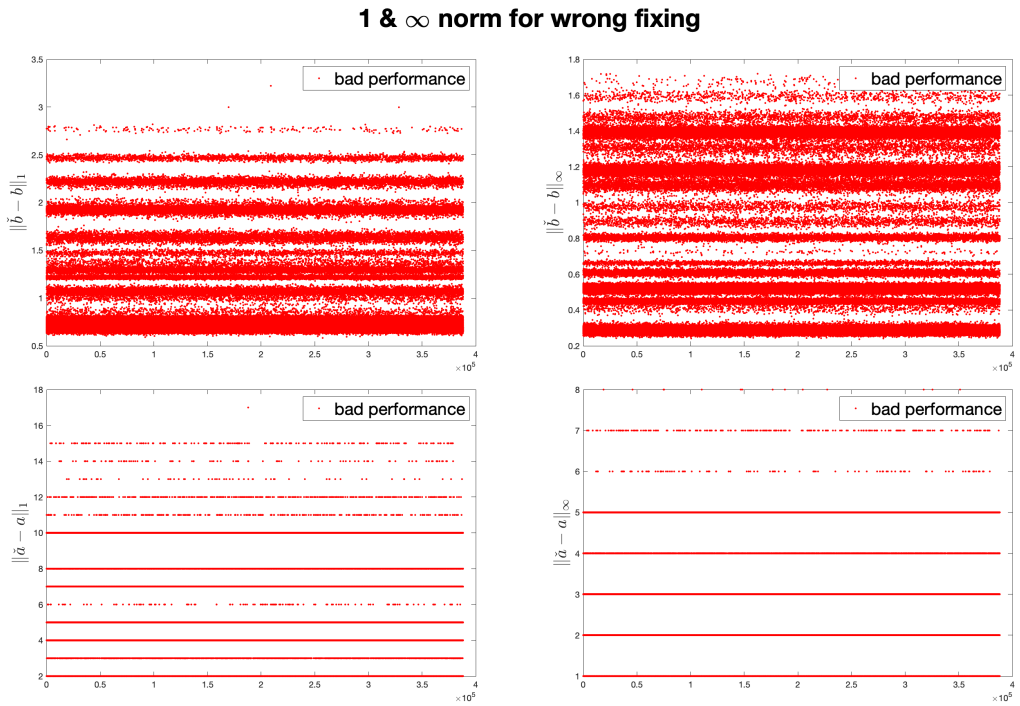

Figure 3.5: Sequences of 1-norm or infinity-norm for wrong baseline or ambiguity residuals, separated by good performance (greed dot) and bad performance (red)

solutions improves over time. It performs much better in dual-frequency scenario. And in our scenarios, the performance of wrongly fixed solutions is always bad, which means the testing method works well. Our 4 validation methods also work, with $P_m = 0$ all the time. Besides, as we mentioned at the end of Chapter 2, if we define a relatively not strict good performance, we could also observe some potential wrong fixings that might be accepted around the center area in the third plot of Figure 3.3.

3.5. Extra Experiment: A Scenario Enrolling Atmospheric Delays

Since what we do in above sections are all based on the short baseline scenarios, the atmospheric delays could be neglected. It would be proper to do an extra experiment based on a scenario enrolling the troposphere and ionosphere errors, to see if there exists any difference.

The model we choose is called 'The Ionosphere-weighted GPS Model', which applies a prior information for the ionosphere delays as stochastic corrections[2]. And based on a linear relationship between prior precision of ionospheric delays and length of baseline (3.10) [2], we assume a 3 km baseline scenario with 1 mm prior standard deviation of ionosphere errors, using dual frequencies. Besides, the delay in troposphere is estimated as a parameter without any prior information, and other settings are the same as before.

$$\sigma_I[cm] = 0.04 \cdot l[km] \tag{3.10}$$

For a certain epoch 285, some results could be shown as Table 3.1. As for the probabilities mentioned in (1.13), we separate $P(\|\check{\mathbf{b}} - \mathbf{b}\|^2_{\mathbf{Q}_{\check{b}\check{b}}} \leq \beta^2)$ and $P(\|\hat{\mathbf{b}} - \check{\mathbf{b}}\|^2_{\mathbf{Q}_{\hat{b}\hat{b}}} \leq \beta^2)$ into two types: with or without atmospheric parameters. We use the original one to represent the former and $P(\|\check{\mathbf{b}}_\mathbf{I} - \mathbf{b}_\mathbf{I}\|^2_{\mathbf{Q}_{\check{b}\check{b}_\mathbf{I}}} \leq \beta^2)$ & $P(\|\hat{\mathbf{b}}_\mathbf{I} - \check{\mathbf{b}}_\mathbf{I}\|^2_{\mathbf{Q}_{\hat{b}\hat{b}_\mathbf{I}}} \leq \beta^2)$ to represent the later. Table 3.1 shows some difference, especially the **RD** method, that a set of loose thresholds fail to detect and validate the wrong fixing in this scenario. In details, Figure 3.11 shows what causes the difference, that in this scenario, the joint distribution of ambiguities and baseline parameters is more irregular, and even a large residual of ambiguity could lead to a small error of baseline parameters, which is not the case in former scenarios. In other words, the error of fixing using standard **LAMBDA** method is more random than short baseline scenarios. For other 3 methods of detection, they have similar performance as before, while we need to do some adjustments for the threshold to achieve an ideal result.

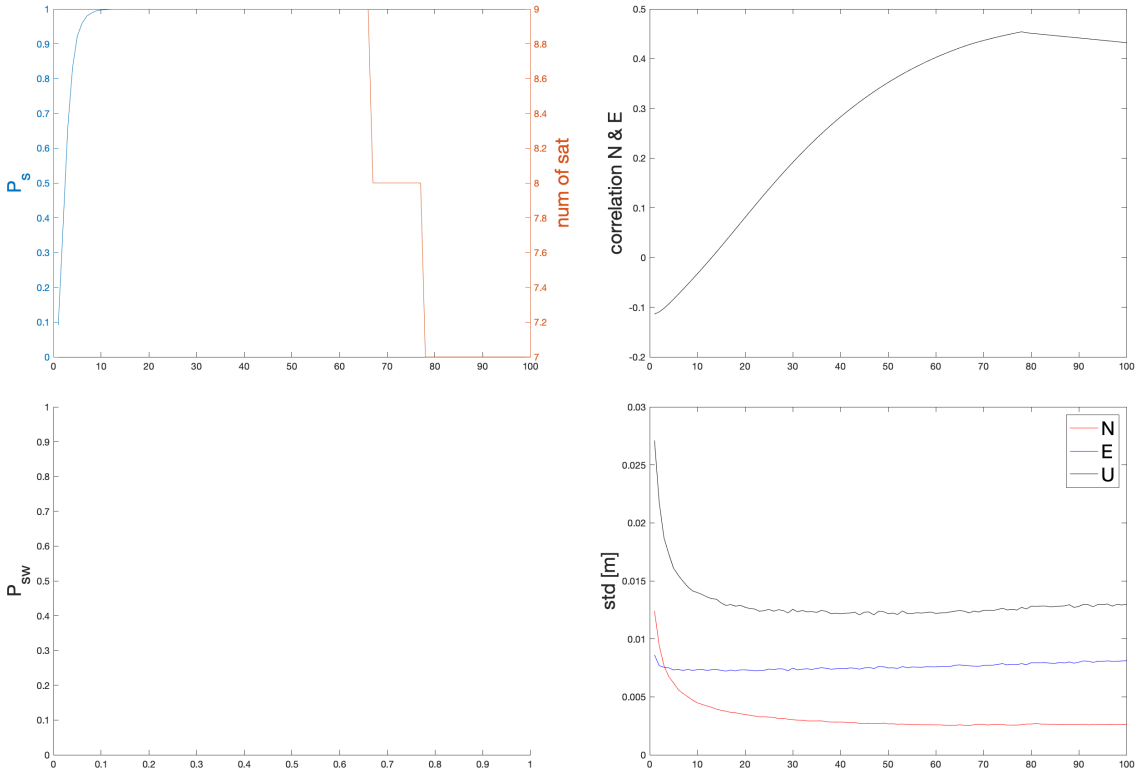

Figure 3.6: Time series of P_s, P_{sw}, number of satellites, horizontal correlation and standard deviation in N, E & U for single frequency with applying Kalman filter

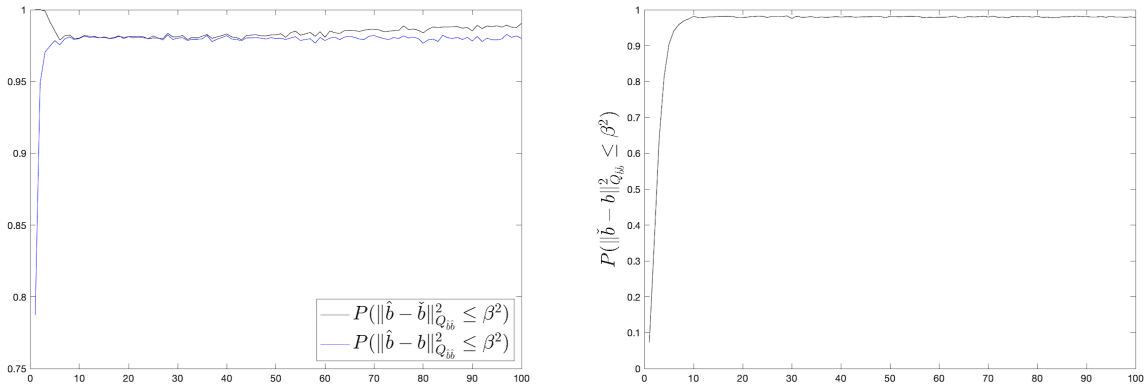

Figure 3.7: Time series of $P(\|\check{\mathbf{b}}-\mathbf{b}\|^2_{\mathbf{Q}_{\check{\mathbf{b}}\check{\mathbf{b}}}} \leq \beta^2)$ $P(\|\hat{\mathbf{b}}-\mathbf{b}\|^2_{\mathbf{Q}_{\hat{\mathbf{b}}\hat{\mathbf{b}}}} \leq \beta^2)$ and $P(\|\hat{\mathbf{b}}-\check{\mathbf{b}}\|^2_{\mathbf{Q}_{\hat{\mathbf{b}}\hat{\mathbf{b}}}} \leq \beta^2)$

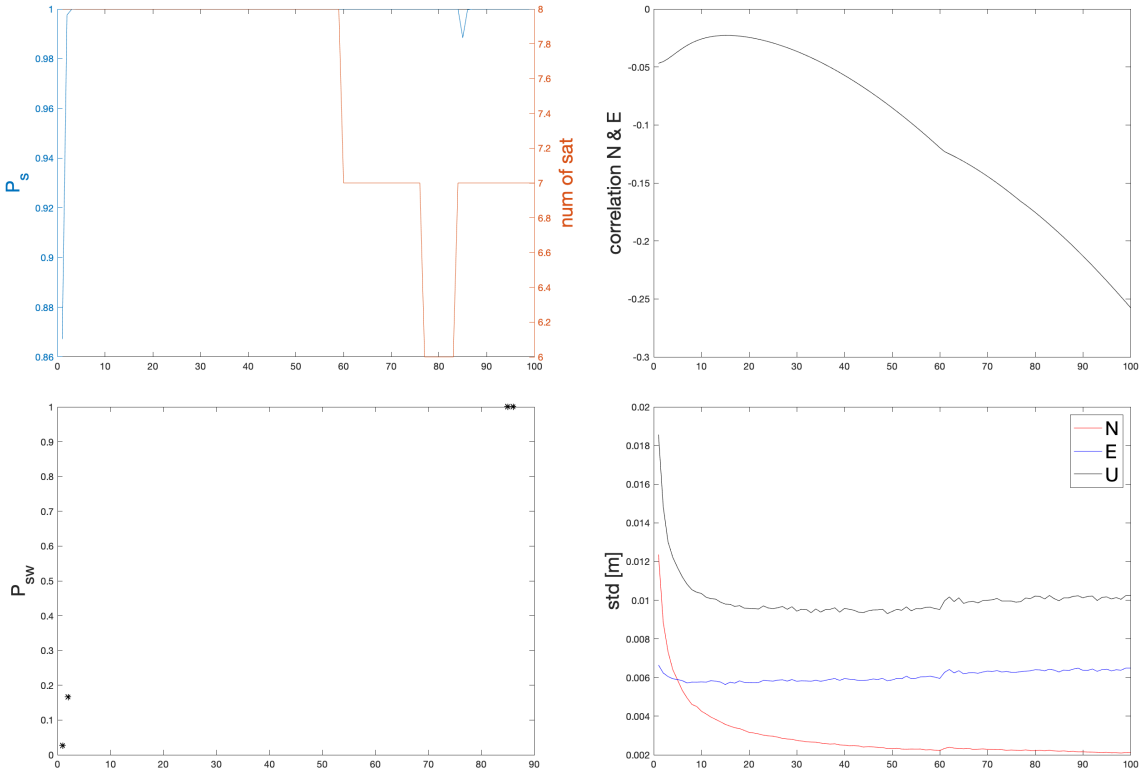

Figure 3.8: Time series of P_s, P_{sw}, number of satellites, horizontal correlation and standard deviation in N, E & U for dual frequencies with applying Kalman filter

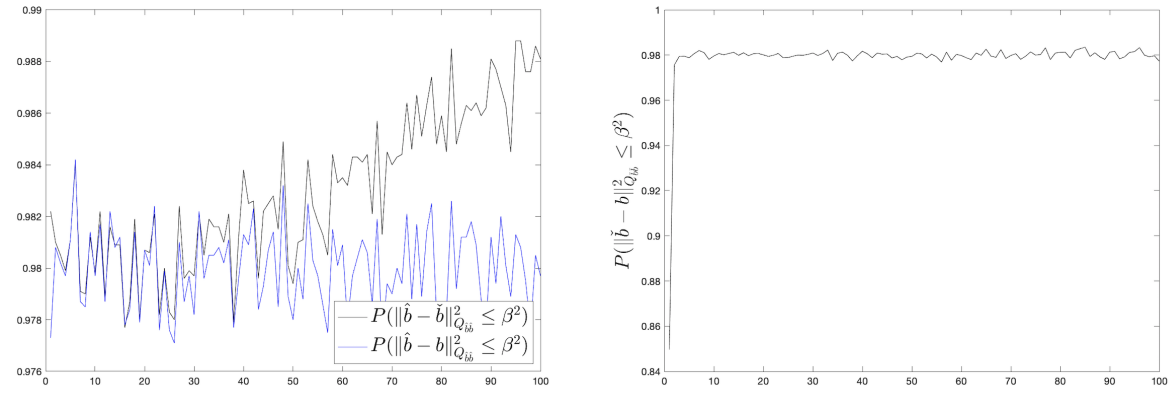

Figure 3.9: Time series of $P(\|\check{\mathbf{b}}-\mathbf{b}\|^2_{\mathbf{Q}_{\check{\mathbf{b}}\check{\mathbf{b}}}} \leq \beta^2)$ $P(\|\hat{\mathbf{b}}-\mathbf{b}\|^2_{\mathbf{Q}_{\hat{\mathbf{b}}\hat{\mathbf{b}}}} \leq \beta^2)$ and $P(\|\hat{\mathbf{b}}-\check{\mathbf{b}}\|^2_{\mathbf{Q}_{\hat{\mathbf{b}}\hat{\mathbf{b}}}} \leq \beta^2)$ between timestep 1-100

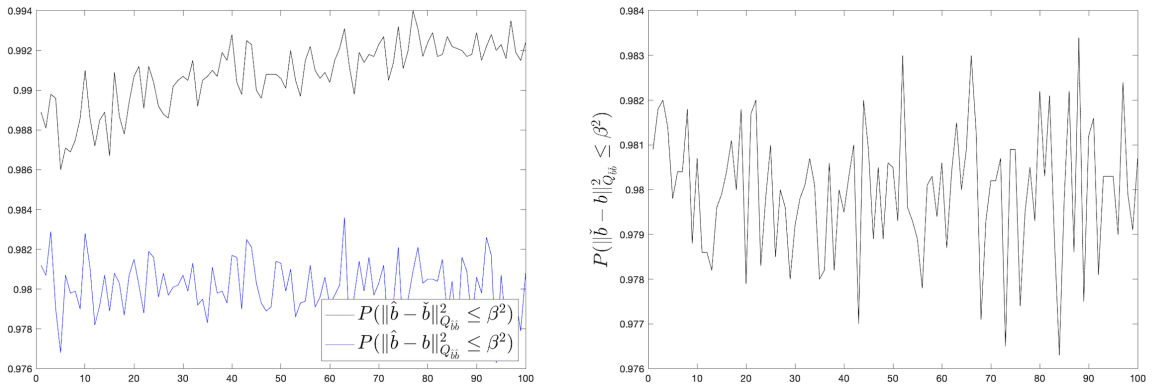

Figure 3.10: Time series of $P(\|\check{\mathbf{b}}-\mathbf{b}\|^2_{\mathbf{Q}_{\check{\mathbf{b}}\check{\mathbf{b}}}} \leq \beta^2)$ $P(\|\hat{\mathbf{b}}-\mathbf{b}\|^2_{\mathbf{Q}_{\hat{\mathbf{b}}\hat{\mathbf{b}}}} \leq \beta^2)$ and $P(\|\hat{\mathbf{b}}-\check{\mathbf{b}}\|^2_{\mathbf{Q}_{\hat{\mathbf{b}}\hat{\mathbf{b}}}} \leq \beta^2)$ between timestep 101-200

In terms of time series, similarly we apply the Kalman filter to see the improvements. Starting from epoch 200, results are shown as Figure 3.12 and 3.13. There is a huge decrease of standard deviation in up direction at the first 10 time steps, and the final result is very close to the short baseline scenario with dual frequencies ($\sigma_N \doteq 2mm, \sigma_E \doteq 5mm, \sigma_U \doteq 1cm$), which also prove the reliability of Kalman filter. $P_{sw} = 0$ means it is less likely to generate good performances in a relatively not complicated scenario (our scenario is simple with length of 3 km baseline only). As for the probability $P(\|\hat{\mathbf{b}}-\check{\mathbf{b}}\|^2_{\mathbf{Q}_{\hat{\mathbf{b}}\hat{\mathbf{b}}}} \leq \beta^2)$ and $P(\|\hat{\mathbf{b}}_\mathbf{I}-\check{\mathbf{b}}_\mathbf{I}\|^2_{\mathbf{Q}_{\hat{\mathbf{b}}\hat{\mathbf{b}}_\mathbf{I}}} \leq \beta^2)$, the later has a more obvious trend of increase, which shows that other than baseline parameters, residuals of atmospheric parameters also decrease a lot during filtering. And other three kinds of probabilities converge to certain constants.

Epoch	P_s	P_{sw}	$P(\|\check{\mathbf{b}}-\mathbf{b}\|^2_{\mathbf{Q}_{\check{\mathbf{b}}\check{\mathbf{b}}}} \leq \beta^2)$ $P(\|\check{\mathbf{b}}_\mathbf{I}-\mathbf{b}_\mathbf{I}\|^2_{\mathbf{Q}_{\check{\mathbf{b}}\check{\mathbf{b}}_\mathbf{I}}} \leq \beta^2)$	$P(\|\hat{\mathbf{b}}-\mathbf{b}\|^2_{\mathbf{Q}_{\hat{\mathbf{b}}\hat{\mathbf{b}}}} \leq \beta^2)$	$P(\|\hat{\mathbf{b}}-\check{\mathbf{b}}\|^2_{\mathbf{Q}_{\hat{\mathbf{b}}\hat{\mathbf{b}}}} \leq \beta^2)$ $P(\|\hat{\mathbf{b}}_\mathbf{I}-\check{\mathbf{b}}_\mathbf{I}\|^2_{\mathbf{Q}_{\hat{\mathbf{b}}\hat{\mathbf{b}}_\mathbf{I}}} \leq \beta^2)$
285	50.99%	2.74%	50.00%, 49.58%	96.07%	98.95%, 99.37%
Method	Threshold	P_{par}	P_d	P_m	$\gamma = P_m/(P_d P_{sw})$
RD	0.15	98.03%	12.98%	18.55%	52.06
	0.11	80.68%	16.06%	11.90%	27.01
	0.07	51.78%	28.85%	3.60%	4.55
WD	27.93	100.00%	79.23%	0.74%	0.34
BD1	0.18	99.72%	90.57%	0.29%	0.12
BDi	0.15	97.75%	92.36%	0.23%	0.09

Table 3.1: Some statistics for validation in epoch 285

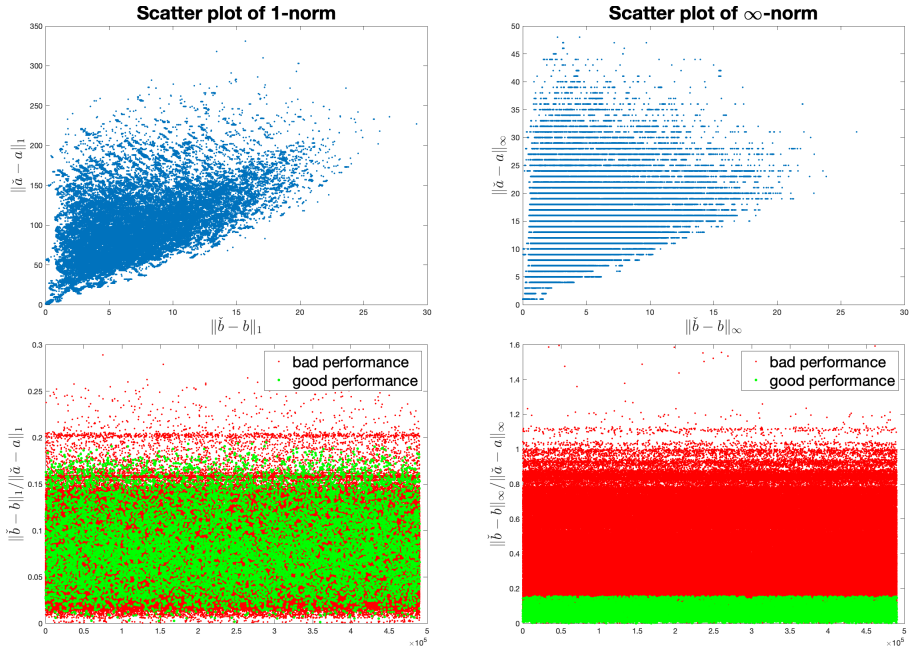

Figure 3.11: Top two are scatter plots of the 1-norm and infinity-norm of residuals for wrong ambiguity vs. baseline, and bottom two are sequences of corresponding ratios between wrong baseline and ambiguity residuals, separated by good performance (green dot) and bad performance (red dot)

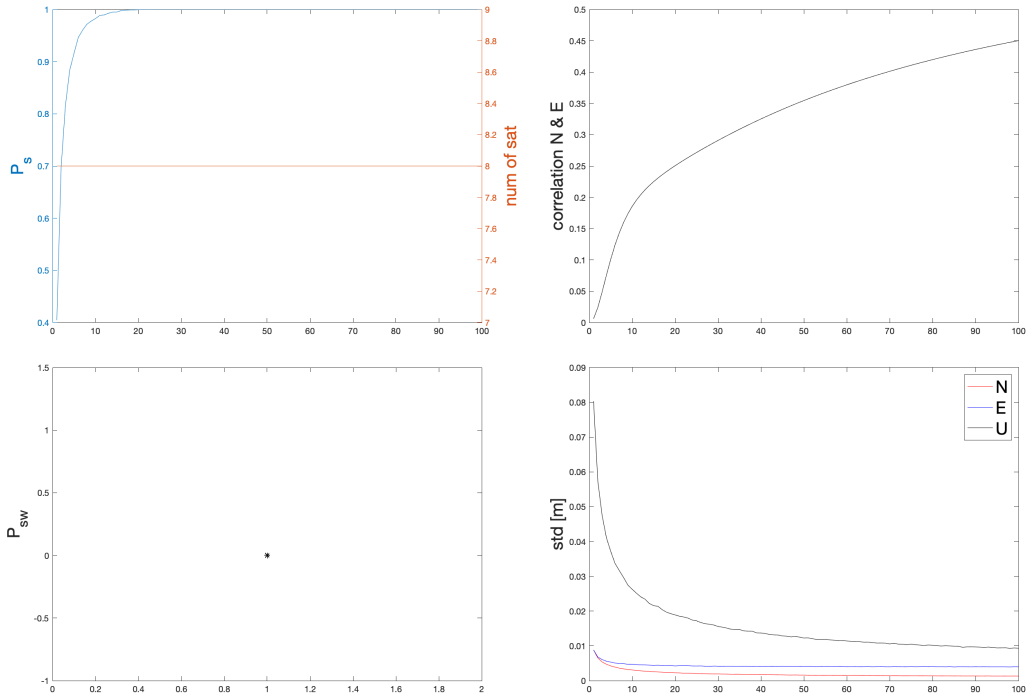

Figure 3.12: Time series of P_s, P_{sw}, number of satellites, horizontal correlation and standard deviation in N, E & U for single frequency with small standard deviation

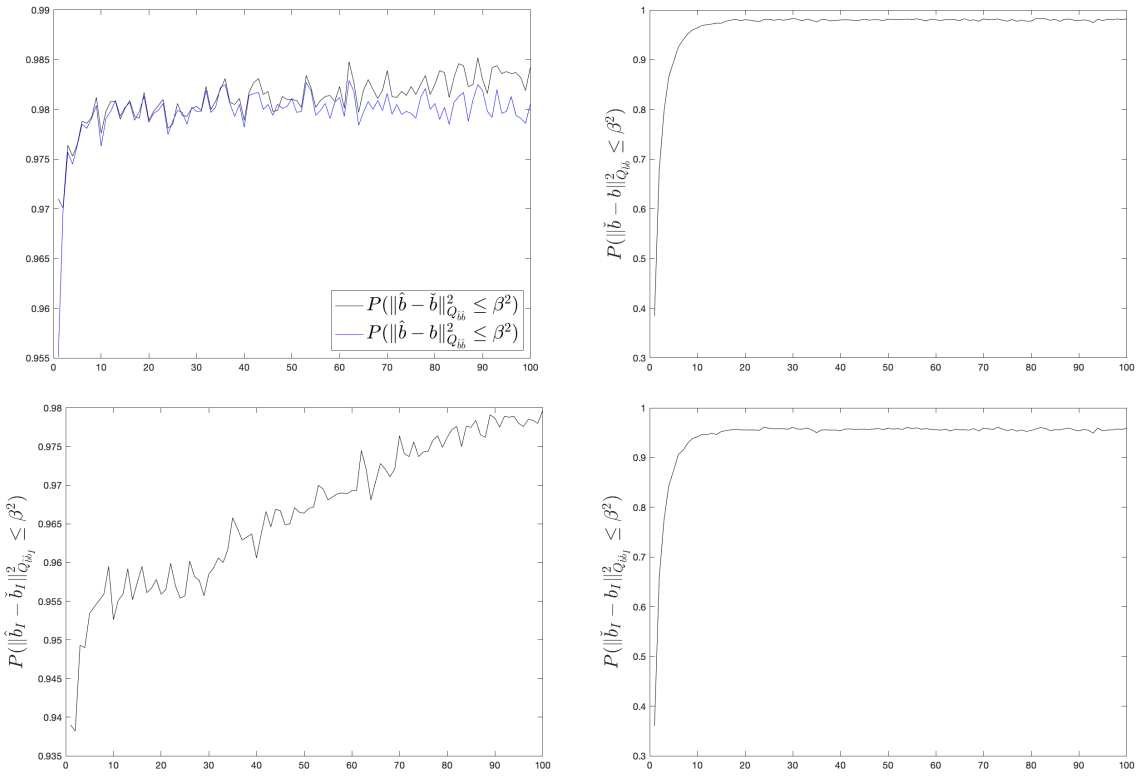

Figure 3.13: Top two figures are time series of $P(\|\check{\mathbf{b}}-\mathbf{b}\|^2_{\mathbf{Q}_{\check{\mathbf{b}}\mathbf{b}}} \leq \beta^2)$ $P(\|\hat{\mathbf{b}}-\mathbf{b}\|^2_{\mathbf{Q}_{\hat{\mathbf{b}}\mathbf{b}}} \leq \beta^2)$ and $P(\|\hat{\mathbf{b}}-\check{\mathbf{b}}\|^2_{\mathbf{Q}_{\hat{\mathbf{b}}\check{\mathbf{b}}}} \leq \beta^2)$; bottom are $P(\|\check{\mathbf{b}}_\mathbf{I}-\mathbf{b}_\mathbf{I}\|^2_{\mathbf{Q}_{\check{\mathbf{b}}\check{\mathbf{b}}_\mathbf{I}}} \leq \beta^2)$ and $P(\|\hat{\mathbf{b}}_\mathbf{I}-\check{\mathbf{b}}_\mathbf{I}\|^2_{\mathbf{Q}_{\hat{\mathbf{b}}\hat{\mathbf{b}}_\mathbf{I}}} \leq \beta^2)$

4

Conclusion and Outlook

In this research we analyse the impact of the wrong fixing in different positioning scenarios with a simulation-based method, using **LAMBDA** toolbox. Starting from a simple case then we visualize some details of wrong fixings and develop 4 methods for the validation. We also check the reliability of each validation method, as well as the bounds of float or fixed solutions in time series under different parameters. Finally we apply the Kalman filter to see how it improves the bounds, the performance of wrong fixings, etc.

At the beginning, we do some pre-research for the wrong fixing from a intuitive visualization of horizontal residuals as well as some statistics such as success rate and failure rate, while it is a bit tricky to retrieve enough information for the performance in case of wrong fixings. So we define several scenarios under single or dual frequencies, different combinations of standard deviation of code and phase, with or without atmospheric delays, then apply Least-square estimation (**LSE**) to generate variance-covariance matrix of float and fixed solutions in some epochs, based on which we could simulate the float solution under a large sample size (10^6), and fix it by **LAMBDA** method. Then it enables us to compute and plot some statistics we are interested in.

After defining good and bad performance of fixings and some parameters (norms, norm ratios, weighted residual squares) as well as visualizations of the distribution of wrong fixings such as histograms, scatter plots, we notice that we could set a threshold for some parameters to validate the performance of wrong fixings. As we take a simulation-based method, the threshold could be chosen based on the true value, namely the statistical properties of the good performance. And we could generate a relatively large sample of the wrong fixing by increasing the standard deviation of code and phase, which is very easy to do in simulation. We mainly focus on 4 defined methods: **Infinity-norm ratio detection** (**RD**), **Weighted 2-norm detection** (**WD**), **1-norm baseline residual detection** (**BD1**) and **Infinity-norm baseline residual detection** (**BDi**), with also 4 kinds of output for each method:
the success rate of detection $P_d = P(detected\ good\ in\ wrong\ fix.|detected\ good\ \&\ bad\ in\ wrong\ fix.)$,
the rate of misdiagnose $P_m = P(detected\ bad\ in\ wrong\ fix.|bad\ in\ wrong\ fix.)$,
the rate of participation $P_{par} = P(detected\ good\ in\ wrong\ fix.|good\ in\ wrong\ fix.)$, $\gamma = \mathbf{P_m}/(\mathbf{P_d}\cdot\mathbf{P_{sw}})$.
Besides, we also calculate 3 kinds of probabilities: $P(\|\check{\mathbf{b}}-\mathbf{b}\|^2_{\mathbf{Q}_{\hat{b}\hat{b}}} \leq \beta^2)$, $P(\|\hat{\mathbf{b}}-\mathbf{b}\|^2_{\mathbf{Q}_{\hat{b}\hat{b}}} \leq \beta^2)$ and $P(\|\hat{\mathbf{b}}-\check{\mathbf{b}}\|^2_{\mathbf{Q}_{\hat{b}\hat{b}}} \leq \beta^2)$ for short baseline scenarios and 2 extra kinds of probabilities: $P(\|\check{\mathbf{b}}_\mathbf{I}-\mathbf{b}_\mathbf{I}\|^2_{\mathbf{Q}_{\hat{b}\hat{b}_\mathbf{I}}} \leq \beta^2)$ and $P(\|\hat{\mathbf{b}}_\mathbf{I}-\check{\mathbf{b}}_\mathbf{I}\|^2_{\mathbf{Q}_{\hat{b}\hat{b}_\mathbf{I}}} \leq \beta^2)$ for scenario enrolling atmospheric delays, all of which are based on (1.13), to check if the wrong fixing is well bounded. Then we extend our experiments from focusing on some epochs to epochs on a whole day for time series analysis, to get an overall concept of performance of difference validation methods, as well as the distribution of P_{sw}, P_s, standard deviation of baseline parameters.

Finally, we apply the multi-epoch **LSE** and Kalman filter to see how these methods could improve the fixing solution, and compute similar statistics as before.

Overall, it is clear that smaller standard deviations of code and phase measurements are ideal for us in practice since very few wrong fixings are generated in this kind of scenario. While in fact it is difficult to keep the environment well for observations all the time, and it would be always the case that code or phase is not precise enough in some epochs. As a result, we cannot neglect wrong fixings and need to do the validation if the success rate of fixing is not high enough.

For scenarios in single and dual frequencies, the standard **LAMBDA** method works well in scenarios of single frequency under short baseline, so we do not need to do the validation for the wrong fixing, which means wrong fixings are all labeled as bad performance in this case. While in some cases like long baseline positioning we seldom use single frequency since the precision of result would be very low. Using dual frequencies could increase the success rate of fixing remarkably, while in some epochs, part of wrong fixings could be accepted due to the small residual of baseline parameters. But it is still a very random case for which epoch there exists $P_{sw} > 0$. And a large sample size of the wrong fixing does not mean there exists good performance. As a result, the validation method is very important to help us label our wrong fixings as good or bad performance.

In terms of 4 validation methods we have mentioned, they work well in short baseline scenarios if we find proper threshold. And if we cannot make sure whether the threshold is reliable or not, it is better to apply a tight threshold to exclude misdiagnoses as many as possible since we need to prioritize the accuracy of our validation methods. In real-time processing, we need some prior information to compute a set of thresholds for the validation, or we start with a strict threshold then adapt its value during the processing. The **RD** method fail to work in scenario enrolling atmospheric delays because of more random residual in ambiguity, which also shows that **LAMBDA** method is less and less reliable with more and more complicated environment.

For time series analysis, the standard deviation, the bound of residuals of baseline parameters are all related to the success rate of fixing, that a high success rate could mean that the standard deviation of detrended baseline parameters is small and their residuals are well bounded, namely the probabilities we compute are very high, while P_{sw} is randomly distributed and suffers from accidental error because of the small sample size in some epochs. In addition, under a constant threshold, the performance for a certain validation method varies in different epochs, but usually it performs well, especially using a tight threshold. A limitation of time series analysis is that it is time-consuming to generate an ideal time series with large enough sample size, leading to some anomalies in our figures. So the result in some epochs with very high success rate is not accurate enough because less wrong fixings are generated .

Finally, the improvement of Kalman filter is very obvious for the success rate, the bounds and the standard deviation especially in up direction. And so does the visualization in horizontal errors. Besides, there is also an improvement of float baseline solution during filtering. But due to the fact that the result from Kalman filter could converge within about 10 time steps in our cases, we cannot observe many epochs when $P_{sw} > 0$, even there is no such epoch. And time series of result from Kalman filter also suffers from the limitation we have mentioned before. But in practice it might take much longer time for the filtered result to converge, especially for Precise Point Positioning (**PPP**), which means it is still possible to find many epochs with $P_{sw} > 0$ before convergence.

In Section 1.4 we pose some questions and now we could answer them:

1. **the bounds of float or fixed solutions**: the float or fixed solution is well bounded if the fixing success rate P_s is high enough (larger than about 95%);

2. **how many wrong fixings could be accepted and how to accept them**: we use 4 different methods **RD**, **WD**, **BD1**, **BDi** for validation and they work well in most scenarios. While we need to find a more proper threshold in a relatively complicated scenario to make sure our validation methods could work. As for the percentage of wrong fixings with good performance among all wrong fixings P_{sw}, it is very random in different epochs, as well as in different scenarios;

3. **how to retrieve the feature of wrong fixings**: we use a simulation-based method to generate a larger sample of wrong fixings under a relatively large standard deviations of code and phase measurements. Also we define some parameters, compute some statistics such as norms and ratios, and visualize the residual or defined parameters in histograms or in horizontal flat to retrieve some useful information that might help for the validation;

4. **impact under different parameters or estimation methods**: few wrong fixings could be accepted in short baseline positioning with single frequency or applying Kalman filter, and the improvement of Kalman filter is obvious when fixing success rate is low at the beginning. During the day, results from **LSE** also change a lot in different epochs. Besides, atmospheric delays would interrupt a lot for our validation since the ambiguity fixing is very random.

In general, in practice the environment is much more complex, and if we want to improve the validation result, on the one hand we need to define more scenarios to find the regularization or relationship between

the selection of threshold and different scenarios; on the other hand there might exist more effective methods. Besides, we could also derive some other fixing methods, as we have mentioned in Chapter 1, to make the fixing solution more reliable.

Bibliography

[1] Mathematical Geodesy and Positioning, TU Delft, GNSS Research Centre, Department of Spatial Sciences, Curtin University. LAMBDA_v3.0 Toolbox, 2012.

[2] D. Odijk. Weighting ionospheric corrections to improve fast gps positioning over medium distances. *ION GPS*, pages 1113–1123, 2000.

[3] P. J.G. Teunissen, O. Montenbruck. *Springer Handbook of Global Navigation Satellite Systems*. Springer International Publishing, 2017. doi: 10.1007/978-3-319-42928-1.

[4] P.De Jonge, C.C.J.M. Tiberius. The LAMBDA method for integer ambiguity estimation: Implementation aspects. *Publ. Delft Comput. Centre LGR-Ser.*, 12:1–47, 1996.

[5] P.J.G. Teunissen, P. Joosten, C.C.J.M. Tiberius. Geometry-free ambiguity success rates in case of partial fixing. In *Proc. ION NTM 1999*, pages 201–207, San Diego (ION, Virginia), 1999.

[6] S. Verhagen, P.J.G. Teunissen. The ratio test for future gnss ambiguity resolution. *GPS Solut.*, 17(4): 535–548, 2013.

[7] P.J.G. Teunissen. Least-squares estimation of the integer GPS ambiguities. Invited Lecture, Section IV Theory and Methodology, IAG General Meeting, Beijing, IAG, Budapest, 1993.

[8] P.J.G. Teunissen. A new method for fast carrier phase ambiguity estimation. In *IEEE PLANS'94*, pages 562–573, Las Vegas, 1994. doi: 10.1109/PLANS.1994.303362.

[9] P.J.G. Teunissen. The invertible GPS ambiguity transformations. *Manuscripta Geodaetica*, 20(6):489–497, 1995.

[10] P.J.G. Teunissen. The least-squares ambiguity decorrelation adjustment: A method for fast GPS integer ambiguity estimation. *J. Geod.*, 70(1):65–82, 1995.

[11] P.J.G. Teunissen. The distribution of the GPS baseline in case of integer least-squares ambiguity estimation. *Artificial Satellites*, 33(2):65–75, 1998.

[12] P.J.G. Teunissen. The probability distribution of the gps baseline for a class of integer ambiguity estimators. *Journal of Geodesy*, 73:275–284, 1999.

[13] P.J.G. Teunissen. The parameter distributions of the integer gps model. *Journal of Geodesy*, 76:41–48, 2002.

[14] S. Verhagen. *The GNSS integer ambiguities: Estimation and validation*. Netherlands Geodetic Commission, 2005.